Modelling borehole flows from Distributed Temperature Sensing data to monitor groundwater dynamics in fractured media

Behzad Pouladi, Olivier Bour, Laurent Longuevergne, Jérôme De La Bernardie, Nataline Simon

Journal Pre-proofs

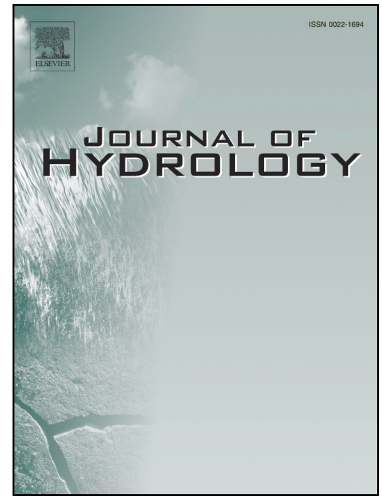

Research papers

Modelling borehole flows from Distributed Temperature Sensing data to monitor groundwater dynamics in fractured media

Behzad Pouladi, Olivier Bour, Laurent Longuevergne, Jérôme de La Bernardie, Nataline Simon

PII: S0022-1694(21)00497-2
DOI: https://doi.org/10.1016/j.jhydrol.2021.126450
Reference: HYDROL 126450

To appear in: *Journal of Hydrology*

Received Date: 3 November 2020
Revised Date: 19 March 2021
Accepted Date: 9 May 2021

Please cite this article as: Pouladi, B., Bour, O., Longuevergne, L., La Bernardie, J.d., Simon, N., Modelling borehole flows from Distributed Temperature Sensing data to monitor groundwater dynamics in fractured media, *Journal of Hydrology* (2021), doi: https://doi.org/10.1016/j.jhydrol.2021.126450

Modelling borehole flows from Distributed Temperature Sensing data to monitor groundwater dynamics in fractured media

Behzad Pouladi *, [1], Olivier Bour[1], Laurent Longuevergne[1], Jérôme de La Bernardie[1], Nataline Simon[1]
[1] Univ Rennes, CNRS, Géosciences Rennes, UMR 6118, 35000 Rennes, France.
Corresponding Author: behzad.pouladi@gmail.com

ABSTRACT

Fractured aquifers are known to be very heterogeneous with complex flow path geometries. Their characterization and monitoring remain challenging despite the importance to better understand their behavior at all spatial and temporal scales. Heat and correspondingly temperature data have gained much interest in recent years and are often used as a tracer for characterizing groundwater flows. In the current work, a fast computer code is developed using Ramey and Hassan and Kabir analytical solutions which converts the temperature profile to the flow rate profile along the borehole. The method developed is validated through numerical simulations. A global sensitivity study recognizes the media thermal properties as the most influential parameters. For testing the method in the field, fiber-optic distributed temperature sensing (FO-DTS) data were used to monitor the dynamic behavior of fractured aquifers at the borehole scale at the Ploemeur-Guidel field site in Brittany, France. DTS data are used to infer the flow rates in the different sections of a fractured wellbore (flow profile) and calculate the contribution of each fracture to the total flow. DTS data were acquired for about three days in three different hydraulic conditions corresponding to two different ambient flow conditions and one pumping condition. Flow profiling using distributed temperature data matches satisfactorily with results from heat-pulse flow metering performed in parallel for cross-checking. Moreover, flow profiling reveals the daily variations of ambient flow in this fractured borehole. Furthermore, it shows that during ambient flowing conditions, shallow and deep fractures contribute roughly equally to the total flow while during the pumping condition, the deepest fractures contribute more to the total flow, suggesting a possible reorganization of flow and hydraulic heads depending on the hydraulic conditions. Thus, although the proposed method (DTS data and proposed framework) may be costlier and is based on indirect characterization through temperature measurements, it provides real-time monitoring of complex fracture interactions and recharge processes in fractured media. Thus, this method allows for a full analysis of the temporal behavior of the system with a simple and fast analytical model. Furthermore, thanks to its narrow width, DTS can be used and installed in boreholes for long-term monitoring while heat-pulse flow metering may lead to head losses in the borehole and may not be always possible depending on some borehole conditions. One of the limitations the approach proposed is the proper knowledge of the thermal properties of media required to infer the flow rate from the temperature. Nevertheless, surface rate measurement can be useful to constrain these properties and reduce the flow profiling uncertainty. Thus, the method proposed appears to be an interesting and complementary method for characterizing borehole flows and groundwater dynamics in fractured media such as for instance, monitoring the recharge dynamic.

KEYWORDS: Fractured media, Borehole Flow, Flow Profiling, Distributed Temperature Sensing (DTS), Heat-Pulse Flow Metering (HPFM)

Nomenclature

Variables

w: Mass rate

H: Enthalpy

v: Fluid velocity

g: Gravitational constant

z: Depth

Q: Heat

T_f : Fluid temperature

T_{ei}: Initial earth temperature

t_d: Dimensionless flow time

t: flow time

k_e : Thermal conductivity of the formation

c_p : Specific heat capacity

c_J : Joule-Thomson coefficient

$f(t_d)$: Time function

L_r : Relaxation distance

GG: Geothermal gradient

U_t: Overall heat transfer coefficient

p: Fluid pressure

r_{wb}: Borehole radius

1. Introduction

Among the established and numerous methodologies used for estimating hydraulic properties in heterogeneous or fractured media (Berkowitz, 2002; Day-Lewis et al., 2017), vertical borehole flow measurement (vertical flow profiling) are often used to characterize fracture connectivity and hydraulic properties (Paillet, 1998; Le Borgne et al., 2006; Day-Lewis et al., 2011). The common practice for vertical borehole flow profiling is performed by using an impeller (Keys, 1990); heat-pulse flow meter (Hess, 1986; Paillet et al., 1987; Le Borgne et al., 2006), or electromagnetic flowmeter (Molz et al., 1994). The two latter methods are particularly interesting for quantifying the relative contribution of the different fractures in ambient conditions to characterize how hydraulic head varies with depths within the borehole (Paillet, 1998). Alternatively, point dilution tracer tests allow obtaining a direct measurement of local groundwater fluxes or Darcy fluxes (Drost et al., 1968; Klotz et al., 1980; Pitrak et al., 2007; Novakowski et al. 2006; Jamin et al. 2015). Nevertheless, the requirement to perform classical dilution tests between packers for characterizing fractured media is a major issue that limits its use in the field.

Some other indirect methods have been developed for vertical borehole flow profiling like for instance dissolved oxygen alteration (Vitale and Robbins, 2017), solute tracers (Michalski and Klepp, 1990), or from the analysis of the temperature profile (Klepikova et al., 2014). Temperature-based methods have been used for a long time in fractured rock hydrology (Silliman and Robertson, 1989; Keys, 1990). The main hypothesis is to assume that if heat advection occurs, due to fracture or borehole flows, the temperature profile should deviate from geothermal gradient that is controlled by heat conduction (Anderson, 2005). Thus, any anomaly or deviation from geothermal gradient can be used to infer fracture locations in the borehole and fracture connectivity (Silliman and Robertson, 1989; Keys, 1990; Pehme et al., 2010; Chatelier et al., 2011). In addition, Klepikova et al. (2011) recently showed that it is possible to deduce vertical flows in a borehole from temperature profiles that present a temperature gradient lower than the geothermal gradient. Their methodology was based on a numerical model of flow and heat transfer at the borehole scale and validated through the use of temperature profiles measured in different hydrogeological conditions. The method has been then extended successfully to propose a three-step inversion approach in which temperature profiles inside the boreholes are used to infer vertical borehole flow profile and the inter-borehole fracture connectivity and transmissivity (Klepikova et al., 2014). Meyzonnat et al. (2018) proposed another approach based on the borehole scale heat budget, which is used for qualitative and quantitative interpretation of depth-temperature data to infer water origin and position of water inflows.

The emergence and promising advances of new temperature sensing technologies such as Distributed Temperature Sensors (DTS) which allows recording temperature along fiber-optic (FO) cables at an unprecedented spatial and temporal resolution, encouraged few authors to develop this technology for fractured rock hydrology (Read et al., 2013). In particular, few authors developed temperature tests, where temperature anomalies are artificially induced, for the characterization of vertical borehole flow profile in fractured aquifers. For instance, Leaf et al. (2012), Sellwood et al. (2015) and Read et al. (2015) used the injection of hot water or an electrical heater to infer water direction and velocities in a borehole in ambient and hydraulically stressed conditions. Read et al. (2014) used distributed temperature sensing (DTS) in combination with an electrically heated DTS cable to quantify vertical flow profile in a borehole. The temperature difference between a heating and non-heating cable was used to infer the fluid velocity variations with depths in the borehole.

Even though these methodologies are appealing and promising, but, to the best of our knowledge, they were not used in ambient conditions to monitor temperature variations and detect some possible flow variations through time. Usually, vertical flow profiling is used at a given time scale, assuming that measurements are representative of boundaries conditions to infer the distribution of fracture transmissivity along the borehole (Paillet, 1998; Le Borgne et al., 2006; Day-Lewis et al., 2011). Some approaches at monthly or yearly time scales are common for studying annual recharge (Jimenez-Martinez et al, 2013), but are generally based on hydraulic head variations through time that is very integrative. Flow variations may reveal the sensitivity of the aquifer to changes in boundaries conditions that may be associated with groundwater recharge, tides, or other processes. Being able to monitor flow changes may also allow inferring characteristic response times of fractured media at varying depths. Such changes through time may also be crucial for characterizing mixing and biochemical reactivity in fractured media (Bochet et al., 2020).

Here, we are addressing the use of temperature data to monitor all along the borehole groundwater flows variations through time. For doing so, we propose using FO-DTS which provides temperature monitoring at an excellent spatial and temporal resolution. In addition, to provide real-time monitoring of flows at different depths, we are using a framework based on analytical solutions for converting temperature data into flows, which can be much faster compared to numerical simulators while providing satisfactory results. Due to the high frequency of recorded temperature data, a fast interpretation framework is indeed required to capture the dynamic response of the media. In this paper, we intend to show: (i) the potential of using a simple analytical model to infer vertical borehole flows from temperature data, (ii) the advantage and limitations of using DTS data for monitoring temperature changes and infer vertical flow profile changes along the borehole , and (iii) the potential information that the methodology provides to better characterize groundwater dynamics over time and space.

In the following section, we present the theory of the heat transfer model and describe Ramey's and Hassan Kabir's solutions to infer vertical borehole flows from temperature profiles (Ramey, 1962; Hasan and Kabir, 1994). The calculation procedure used in the proposed framework is described in supplementary materials, and a numerical model is used to validate the proposed framework. Then, after having described the field site, the final section of the manuscript describes an application of the approach for monitoring the hydraulic response of a fractured borehole at the Ploemeur-Guidel field site located in Brittany, France.

2. Flow model from the temperature profile

2.1 State of the Art

In petroleum engineering, the works on the concept of flowing well temperature profile prediction date back to nearly sixty years ago (Edwardson et al., 1962; Lesem et al., 1957; Moss and White, 1959) but the pioneering work belongs to Ramey (1962). He proposed a simple analytical solution to predict the temperature profile of single-phase water in an injection well. Later, his analytical model was successfully applied to production wells (Horne and Shinohara, 1979). The model considers steady-state heat transfer inside the borehole while heat transfer from the borehole to the surrounding formation is governed by transient radial conduction. He considered the borehole as a line source and the surrounding earth as an infinite sink in which heat diffusion only occurs in a horizontal plane and vertical heat diffusion is negligible. In Ramey's analytical model, inflow or outflow of the fluid from formation to the borehole or vice versa is not directly considered. However, the inflow/outflow from the borehole can be inferred by estimating the flow, above and below the production/thief zone. The difference will indicate whether the zone is acting as inflow or outflow. The fluid temperature moving inside the borehole is a function of the depth, thermal properties of the borehole, surrounding earth, and also flow time. A time function is introduced to account for the temporal heat transfer behavior in the formation. Later Satter (1965) and Sagar et al. (1991) extended Ramey's model to two-phase flow by taking into account, the effect of the kinetic energy and Joule Thompson effect caused by pressure change along the borehole. Hagoort (2004) examined Ramey's model applicability and found out that it can be an excellent approximation except at early times when the calculated temperature is overestimated.

Hasan and Kabir (1994) further developed Ramey's model. They proposed a new approximate solution for transient heat transfer in the formation as well as incorporating both convective and conductive heat transport for the wellbore/formation system. In Hassan and Kabir's model, they used an appropriate inner boundary condition (finite wellbore) for wellbore/formation heat transfer and demonstrated the importance of including the convective heat transfer. Later, Kabir et al. (1996) proposed a model using energy, mass and momentum balance and including different fluid inflows to the borehole. Afterward, there have been many publications by Hassan et al. incorporated the hydrodynamic of different flow patterns and well geometry (2007, 2002). In one of his most general works, a robust analytical steady-state model is presented which includes wellbore inclination, varying geothermal gradient, and Joule-Thomson effect by dividing the borehole into sections of uniform thermal properties and inclinations (Hasan et al., 2009). The limitation of this approach is that the solution is not applicable in production zones (in front of production zones) but rather in stable flowing zones above and below the production zone.

Ramey (1962) and Hassan and Kabir's (1996) models were mostly applied for applications implying multiphase flows in petroleum engineering, CO_2 sequestration or geothermal energy development. However, Hasan & Kabir's and Ramey's solutions can be applied for hydrological applications. In such a case, the physics of flow and temperature exchanges must be simplified for single-phase flow. No specific assumption would limit the application of these solutions to hydrology. Silva et al. (2019) recently validated Ramey's solution experimentally for a range of water flow rates similar to our application in the field. Using a laboratory prototype, they obtain very good agreement between flow rate measurements derived from temperature profiles using Ramey's model with imposed flow rates (Silva et al., 2019). Preto et al. (2019) investigated the reason for nonlinearity in the recorded geothermal gradient in the upper part of a deep wellbore which could not be explained by the variability of measured thermal properties of sediments and rocks. They also used Ramey's equation to see if the vertical flow of warm fluid in the upper part can explain this discrepancy between measured and modeled geothermal temperature. They estimated the vertical flow velocity and concluded that this discrepancy can be explained by the infiltration of warm fluid transported from depth by fractures (Preto et al., 2019). In this work, the use of Hasan & Kabir's solution for converting temperature profile into flow profile is validated numerically (section numerical validation) and also experimentally by cross-checking the estimated flow rates with measured flow rates by a heat pulse flow meter.

Emergence and promising advances of new temperature sensing technologies such as Distributed Temperature Sensors which allows recording of high spatial and temporal temperature has also encouraged researchers to use these data type in petroleum engineering (Ouyang and Belanger, 2004; Kluth and Naldrett, 2009; Wang, 2012; Kabir et al., 2012; Nuñez-Lopez et al., 2014), especially for flow profiling inside boreholes and characterization of the unconventional reservoirs (Luo et al., 2020a; 2020b). These types of data can provide real-time monitoring of the system which may be very useful, especially when the system is subjected to different natural and artificial hydrological process variations. However, real-time, transient analysis of DTS data may not be practically favorable due to the computational time and resources required. In one of the recent works, Alemán et al. (2018) have used machine learning techniques for flow profiling and calculation of the fracture flow rate using temperature data to assess the effectiveness of the hydraulic fracturing operations in oil and gas wells.

2.2 Heat Transfer Model

This subsection is devoted to briefly explain the heat transfer model developed by Ramey (1962) and Hasan and Kabir (1994) which are used in the current paper. We have provided more explanation of the derivation of equations in Appendix A. We encourage those who are interested in the detailed derivation of the analytical model to refer to works published by these authors as given in the references.

Considering a flowing volume of water in the j[th] section of the wellbore between z and z-dz (Figure 1), both models assume steady-state heat transfer inside the wellbore and transient radial heat transfer from the borehole to the formation. Writing up the energy balance for the control volume, assuming radial heat transfer from the fluid to the surrounding earth, solving the two equations jointly with proper initial and boundary conditions (see Appendix A), we come up with the following equation which describes fluid's temperature profile (T_f) along a vertical borehole depth, z.

$$T_f = T_{ei} + \frac{[1-e^{(z-z_j)L_r}]}{L_r}(GG-\frac{g}{c_p})+[T_{fj}-T_{eij}]e^{(z-z_j)L_r} \quad (1)$$

Here, T_{ei} is the initial earth temperature (the temperature at geothermal gradient), T_{fj} and T_{eij} are fluid temperature and initial earth temperature at the fluid entry point to the borehole (z_j), respectively. Also, GG, g and c_p represent the geothermal gradient, gravitational acceleration, and specific heat capacity of water, respectively. Furthermore, L_r is called the relaxation distance. This is the distance that is required by the fluid to be traveled so the fluid temperature gradient becomes parallel to the geothermal gradient. The relaxation distance is dependent on fluid velocity as well as the thermal properties of the fluid and media.

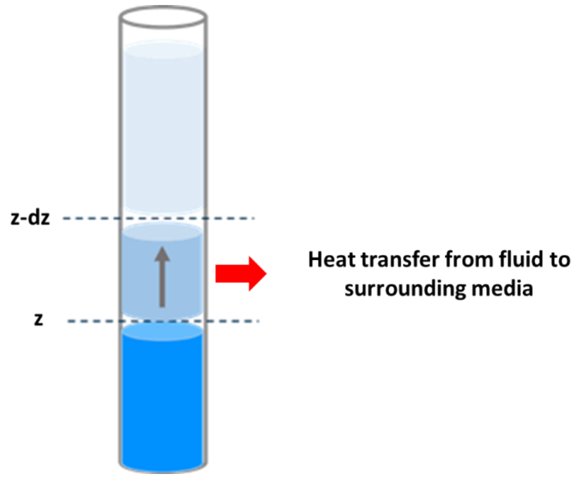

Figure 1: Diagram of the Control Volume used for heat transfer modeling inside the production borehole. Heat is either advected by fluid flow or conducted radially in the surrounding media.

The formula for L_r in Ramey and Hassan Kabir equations are essentially the same but proposed for different boundary conditions assumed for solving the set of equations. Ramey considered the borehole as a line source while Hassan and Kabir defined the borehole as a finite radius boundary condition. However, both solutions converge at late times.

$$L_r^{Ramey} = \frac{wc_p f(t_d)}{2\pi k_e} \tag{2}$$

$$L_r^{Hassan\&Kabir} = \frac{wc_p}{2\pi}\left[\frac{k_e + r_{wb} U_t f(t_d)}{r_{wb} U_t k_e}\right] \tag{3}$$

$$t_d = \frac{k_e t}{r_{wb}^2} \tag{4}$$

$$f(t_d) = \ln(1 + 1.7\sqrt{t_d}) \tag{5}$$

In the above equations, k_e , r_{wb}, w, c_p are thermal conductivity of the rock, borehole radius, fluid mass rate, and fluid specific heat capacity, respectively. Also t is the flow time, t_d is dimensionless flow time defined in the equation (4). Flow time refers to the time that the borehole has been producing and heat being transferred from the fluid to the surrounding media. The dimensionless time function is shown by $f(t_d)$ accounts for unsteady-state heat transfer to the formation. Furthermore, U_t is the overall heat transfer coefficient which is explained comprehensively in Appendix A. Various forms of formulas for $f(t_d)$ existing in the literature, has been studied and compared by Satman and Tureyen (2016). They suggested that the dimensionless time function by Kutun et al. (2014) as given in equation (5) would be sufficiently accurate for engineering purposes for most values of flow time. This approach is frequently used in petroleum engineering as well as in geothermal reservoir (Nian et al., 2018; Song et al., 2018; Wang., 2019). In the following, we demonstrate its applicability in hydrology by performing numerical validation and also showing its field application.

2.3 Inversion of temperature data and flow profiling

In this section, we explain how distributed temperature data (acquired along the borehole), are used to obtain the water velocity (and consequently water flow rate) in different sections of the borehole. Assuming proper knowledge of the water and media thermal properties (geothermal gradient, the thermal conductivity of the rock, flow time, etc.), L_r is determined so as the recorded distributed temperature data matches the predicted distributed temperature data by minimizing the following objective function. This objective function is the root mean square error normalized by the temperature measurement error variance (temperature accuracy) and minimization continues until the objective function converges to values close to one which means the prediction is within the error level.

$$\text{objective function}=\frac{\sqrt{\sum\frac{(T_{recorded}-T_{predicted})^2}{n}}}{\sigma_{error}} \tag{6}$$

where n and σ_{error} are the number of recorded temperature data and error of recorded temperature data, respectively. Once L_r is determined, we use the Hassan and Kabir equation for the relaxation distance given by equation (3) to calculate the water mass and thus flow rate and water velocity. It should be noted we use equation (3) as it applies to more general cases. In early times, the wellbore is not acting as a line source, so that Ramey's assumption is not satisfied. However, both equations (equations 2 and 3) can also be used to calculate the water flow rate and both should yield the same results for the large flow time and small borehole radius (large values of t_d) as the condition becomes closer to the line source assumption for the borehole.

The minimization process starts with an initial guess L_r. To speed up the minimization process, we need to provide an initial guess close to the final value. For this reason, we use the linearized form of the equation (1) (please see supplementary materials). Using $L_r^{\ Ramey}$ proposed by Ramey, we obtain the following simple equations to estimate the water velocity. This gives us most of the time, a fairly close initial guess to the final solution. The initial guess is given as follow:

$$\left.\frac{dT_{fj}}{dz}\right|_{z=0}=(T_{fj}-T_{ej})\times L_r^{\ Ramey} \tag{7}$$

$$v_{initial}=\frac{2\pi k_e}{\rho_w c_p f(t_d)}\times\frac{T_{fj}-T_{ej}}{\left.\frac{dT_{fj}}{dz}\right|_{Z_j=0}} \tag{8}$$

Here, ρ_{water} and $v_{initial}$ are water density and an initial guess for water velocity, respectively. The above equation simply states that the fluid velocity is not dependent on the absolute value of the temperature but rather on the spatial change of fluid temperature along the borehole.

It should be noted that for multiple flowing zones (different j sections) i.e. zones with different water flow rates in the borehole, we repeat the same procedure explained above. Once the water flow rate in all zones is determined, the contribution of each fracture to the total flow can be inferred from deducing the flow rates in consecutive zones.

2.4 Numerical Validation

2.4.1 Description of the numerical model

A numerical model describing heat transfer of moving fluid from the borehole to the surrounding area has been developed using the finite element-based software COMSOL Multiphysics® v. 5.4. (2018). The model mimics an artesian borehole in which, flow from the bottom of the borehole and flow from different fractures contribute to the total upward flow. This model is used in the following, to first validate the approach and secondly, evaluate the accuracy of the proposed framework. The model calculates fluid temperature profile along the borehole given the thermal properties of the fluid and the media as well as fluid velocity. Then, the generated temperature profile is used to back-calculate the fluid velocity in the borehole by inversion of generated temperature data (using the aforementioned analytical solutions and calculation procedure by the computer code developed). By comparing the given fluid velocity in the model and the one estimated from temperature data, we can evaluate the accuracy of the methodology. The model has been created for cases where one, two, and three fractures are crossing the wellbore although it could be generalized to more complex cases with more fractures crossing the borehole. In this section, only the case of two fractures is shown, but similar results were obtained with one or three fractures.

It can be argued that the thermal effect of the fluid flow inside a fracture on the temperature distribution in the rock matrix away of the borehole (which consequently affects the fluid temperature inside the wellbore) may not be significant. Thus, to reduce the computational complexity associated with including fractures in the model, the borehole is divided into different sections and different fluid velocity is given to each section as shown in Figure 2. This mimics the presence of fractures and their contribution to the total flow in the borehole. Figure 2 represents the numerical model schematic, meshing, and representation of physic used to model the effect of fracture in the borehole (for a case of two fractures). In the model, the outer radius and height of the aquifer are considered to be 100 m while the borehole radius is chosen as 0.07 m. The mesh size is small around the borehole while being larger moving away toward the boundaries.

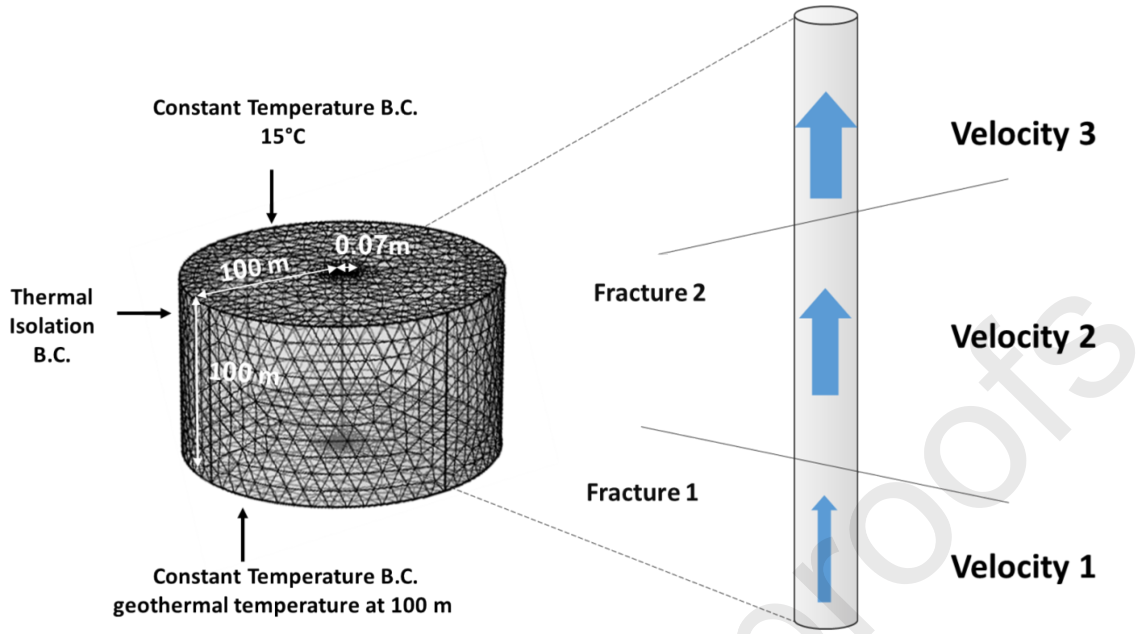

Figure 2: Schematic of the numerical model and representation of the borehole with two fractures and three flowing sections

2.4.2 Synthetic test with two fractures

In this part, it is assumed an artesian borehole in which two fractures are crossing the wellbore at the depths of 100 m and 70 m contributing to the total flow of water. There is a flow from the bottom of the borehole (velocity 1) and two fractures are also contributing to the total flow. The water and rock specific heat capacities are respectively fixed to 4180 and 750 (J/kg×°C) while water and rock densities are respectively 1000 and 2560 (kg/ m^3). The geothermal gradient used in the model is 0.016 (°C/ m), as proposed by Klepikova et al. (2011) for the same site chosen for the application (see section 3). However, the choice of these parameters in the numerical model does not affect the results as they are supposed to be known (the same parameter are used in the computer code). The outer boundary conditions are taken to be thermal isolation. The surface and bottom boundary conditions are respectively set to a constant temperature of 15°C and the geothermal temperature at 100 Sm.

The difference between the flow rate used in the model and flow rate inferred from the temperature by the analytical approach defines the error. Analysis of the results for a different number of fractures, flow rate as well as a different range of flow time, indicate that errors are less than 10%, even for a very low flow rate which may not be measurable by conventional flow meters. The flow rates tested range from 5.42 lit/min to 542.88 lit/min for different flow time ranging from one day to several weeks. As an example, the best and worst estimate for the case of 5 lit/min are 5.43lit/min and 4.98lit/min corresponding to 9% and 1% errors. For the case of 542.88 lit/min, the best and worst estimates are 541.12 lit/min and 494 lit/min and their associated errors are almost zero and 9%, respectively. These errors are very reasonable errors considering the errors of measurements from flowmeters that also range classically within 10% or more (Paillet et al 1998). Considering reasonable such errors allow validating the use of the analytical model for converting temperature data into flow profile. In Figure 3, we show the flow used in the numerical model (to generate temperature) versus the estimated flow rate (estimated from the temperature using the analytical solution). It should be noted that here we only show the cases with the highest errors (worst estimates) and we still see the good agreement. It is worth mentioning that the source of this error could be the limitation of analytical solutions (due to their assumption during the derivation) in capturing the real physics of the problem but it still provides satisfactory results. The reasonable accuracy of this analytical solution removes the necessity to use numerical models and simulator which may not everyone has access to it. Furthermore, analytical solutions can be programmed in few lines of codes or even simply in an excel sheet.

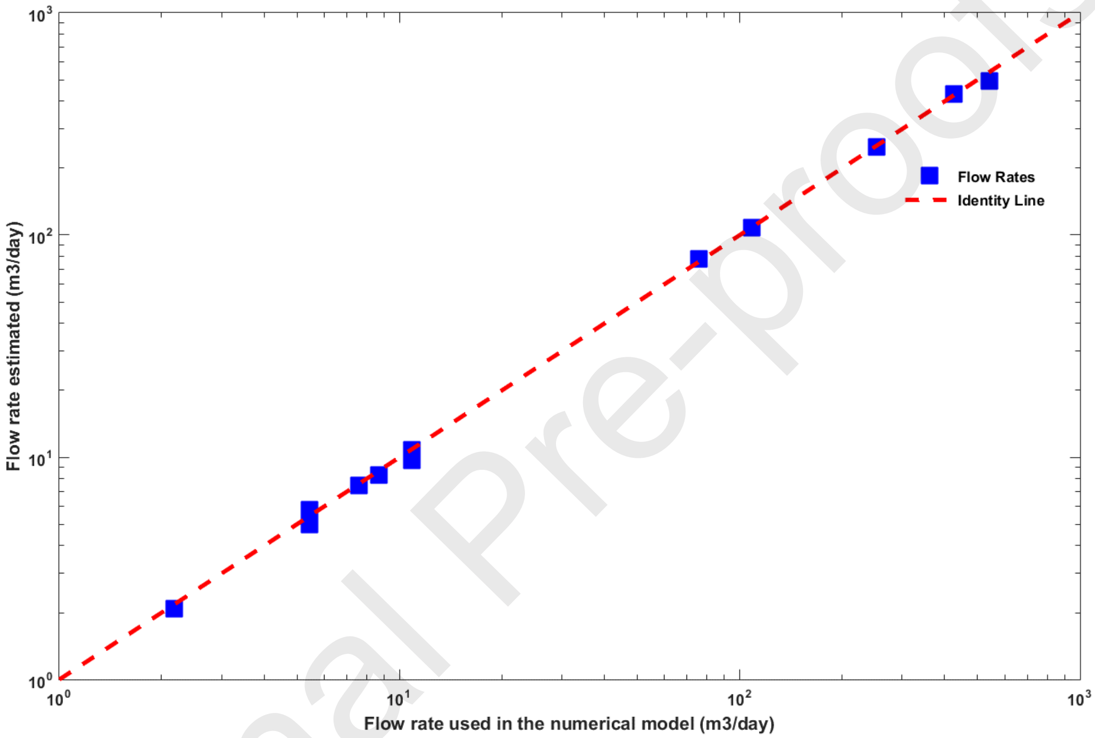

Figure 3: Comparison of flow rate used in the numerical model and flow rate calculated from the temperature data using the analytical approach

2.5 Sensitivity of the model to the different parameters

The analytical model being validated, we investigate here the sensitivity of the model to the different parameters. In the supplementary materials, some simulations are presented to investigate the respective impact of the different parameters. For the hydrological application considered, we found that the three most important parameters are the geothermal gradient, the thermal conductivity of the rock, and the flow time (by order of importance). Indeed, as heat is continuously exchanged between borehole and media with time, near-wellbore region will equilibrate toward fluid's temperature and heat transfer rate decreases. In fact, the geothermal gradient and flow time determine the driving force while the thermal conductivity of the rock controls the heat transfer rate.

To complement this analysis, a global sensitivity analysis has been performed using the Sobol method available in the safe MATLAB toolbox (Pianosi et al., 2015). It allows determining the importance of the most influential parameters on the calculated flow rate. In a global sensitivity analysis, all parameters are varied simultaneously over the entire parameter space, which leads to simultaneously evaluate the relative contributions of each individual parameter as well as the interactions between parameters to the model output variance. To date, several types of global sensitivity analyses have been developed. However, variance decomposition based Sobol sensitivity analysis is so far one of the most powerful techniques. Sobol sensitivity analysis intends to determine how much of the variability in model output is dependent upon each of the input parameters, either upon a single parameter or upon an interaction between different parameters. In order to understand how the output variance can be attributed to individual input variables and the interaction between each of the input variables, the total-order, first-order (main effect), second-order, and higher-order sensitivity indices are calculated to accurately reflect the influence of the individual input and their interactions. The first order Sobol index (main effect), explains the contribution of parameter alone to the output, while the total index (total effect) reflects the relative importance of one input variable and all its interactions with other variables. Here, the values of the first order Sobol index are 0.66, 0.027, and 0.06 for the geothermal gradient, the thermal conductivity of the rock and flow time while the total Sobol index are 0.97, 0.74 and 0.57, respectively. Figure 4, shows and compares the values of these indices. We see that the geothermal gradient is the most significant variable taking into account both its main effect and its interaction with other parameters. Rock thermal conductivity and flow time have a very small main effect. However, their impact on the total variance is notably high (high values of total effect) due to their interaction with other parameters. This means that uncertainty in flow profiling can be significantly reduced by proper measurement of the geothermal gradient which may not be difficult to estimate in comparison to the other parameters. The geothermal gradient can be measured in the wells with stagnant water inside, ensuring no cross flow happening in a section of the borehole. In such boreholes, the change of stagnant water temperature with respect to the depth reflects the value of the geothermal gradient (assuming that water has stayed long enough in the borehole to reach thermal equilibrium with the surrounding media). However, in case of no or little, knowledge of thermal properties, we will show in section 6.1, how to estimate these parameters for flow profiling application using a measured flow rate.

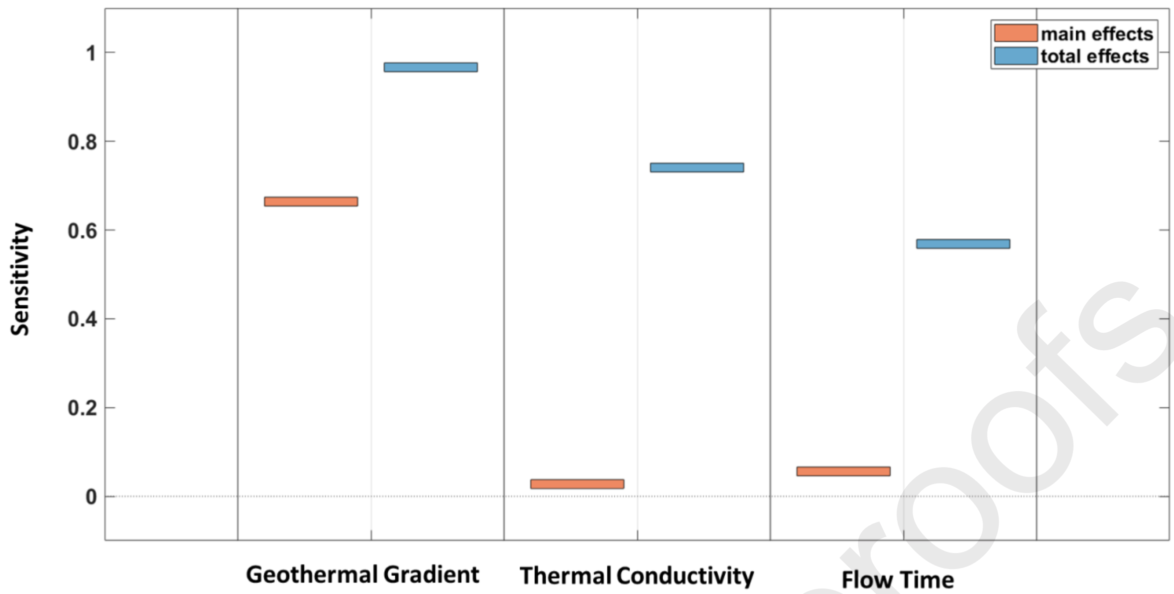

Figure 4: Global sensitivity analysis (Sobol method) performed for three parameters and the corresponding sobol indices including main effect and total effect. The main effect represents the contribution of parameter alone while the total effect represents its interaction with other parameters.

3. Hydrogeological setting

In this section, after having described the Ploemeur-Guidel experimental site, we focus our attention to the borehole chosen to achieve temperature monitoring through DTS and borehole flow profile measurements with Heat-Pulse Flowmeter.

3.1 The Ploemeur-Guidel field site

The field site of Ploemeur-Guidel is a coastal aquifer located in Brittany, France, which provides one million cubic meters of drinking water annually to a nearby town. The mean annual precipitation is about 800 mm while the mean annual evapotranspiration is about 500 mm. Although the site is located in crystalline rocks composed of granite and micaschists, the good connectivity and high hydraulic conductivities of large-scale faults provide water supply since 1991 (Le Borgne et al., 2006). The structural analysis combined with geophysical data (Touchard, 1998; Ruelleu et al., 2010) revealed that the most productive boreholes are located at the intersection of two main tectonic features: a low-angle fault zone between granite and micaschist dipping about 30° to the north, and dextral fault zones regularly spaced and striking north 20°. Compared to other bedrock aquifers in Brittany, this aquifer is outstandingly productive. Although hydraulic properties are highly variable in space, especially at small scales, the large-scale transmissivity of the site varies between 10^{-3} to 10^{-2} m^2/s (Le Borgne et al., 2006; Jimenez-Martinez et al, 2013). The site has been the subject of numerous experiments and studies, which include but are not limited to geophysical imaging, residence times modeling, water chemistry monitoring (Ruelleu et al., 2010; Leray et al., 2012; Roques et al., 2018). The

Ploemeur-Guidel hydrogeological observatory (http://hplus.ore.fr/en/ploemeur) is a part of both the H+ network of hydrogeological sites (http://hplus.ore.fr/en/) and the French Critical Zone network OZCAR (http://ozcar-ri.org/) (Gaillardet et al., 2018). All data used in this study can be found on the H+ database (de Dreuzy et al., 2006; http://hplus.ore.fr/en/).

3.2 Borehole PZ-26

Among the numerous boreholes available, borehole PZ-26 was chosen to experimentally apply the approach. PZ-26 is an artesian borehole located near a small stream and very close to a wetland area fed by groundwater and which is the outlet of the aquifer. The flow rate at the top of the well is varying depending on the seasons. It is maximum after groundwater recharge which occurs in winter in general, while the flow rate is minimum in autumn, just before the start of groundwater recharge. Thus, borehole PZ26 is an artesian well where flows are strongly sensitive to hydraulic changes through time. This sensitivity to hydraulic changes motivated the installation of temperature monitoring through FO-DTS hoping to record flow changes within the borehole through time. Note also that the development of microbial communities that can be observed locally at some fracture intersections up to 60 meters deep in this borehole, is strongly related to flows within the borehole (Bochet et al., 2020). Indeed, the developments of these microbial hotspots appear due to intermittent oxic–anoxic fluid mixing in relation to flow dynamics in the borehole, (Bochet et al., 2020). According to a simple mechanistic model of fluid flow and mixing in fractures, the authors showed that such microbial hotspots are sustained by the mixing of fluids with contrasting redox chemistries at fractures intersections and that meter-scale changes in near-surface water table levels could cause intermittent oxygen delivery through deep fractures (Bochet et al., 2020). Thus, temperature monitoring using FO-DTS was considered a promising tool for monitoring flow changes along the borehole to better understand flow dynamics and microbial communities development. Although the analysis of microbial communities development is beyond the scope of the present study, and the fact that flow profiles from temperature monitoring is an indirect method for estimating borehole flows, the advantage of FO-DTS borehole is to provide flow profiles through time all along the borehole without leading to head losses in the boreholes nor using multi-packers that are complex to use and may strongly alter microbial hotspot developments.

PZ 26 is a 6 inches' diameter open borehole where about a dozen permeable and producing fractures have been identified thanks to optical and flowmeter borehole logging (Bochet et al., 2020). Despite the depth of the borehole, only mica-schists dipping slightly towards the north has been encountered in the borehole. The deepest fractures were found the most productive (below 94m). Fractures in this borehole inherit two different orientations; North-West oriented and East oriented fractures. Note that the golden color shown on the borehole schematic in Figure 5, for depths above 59 meters, corresponds to iron-oxide precipitation that results from the mixing of oxygen-containing surface water and iron-rich deep water. The value of the transmissivity of the productive fractures above 94m in this borehole ranges from 10^{-4} to 5.10^{-4} m^2/s measured by borehole flowmetry (Bochet, 2017).

4. Data acquisition and processing

In this section, we first describe how FO DTS and Heat pulse flow meter were used to obtain data. Then we explain the processing of the data obtained.

4.1 Experimental setting

Distributed Temperature was continuously monitored along the borehole during about three days thanks to a FO-DTS installed in the borehole PZ-26. The FO cable designed by Brugg Kabel AG, Switzerland has a 3.8 mm diameter and is protected by steel armoring and a polyamide jacket. It contains four multimode FOs that were spliced together to make a connection between two FOs. Such splicing allowed double-ended measurement calibration following Van de Giesen et al (2012). The spliced endings were protected by 3-D printed casings filled with epoxy. The end of the cable was easily installed at the bottom of the borehole so that the cable was installed all along the borehole without any tension. DTS data were recorded using a DTS XT unit (Silixa) with a spatial sampling of 25 cm. The cable metering made it possible to associate a depth to each measured temperature. The acquisition frequency was set to every one minute in a double-ended configuration which allows temperature monitoring at a high temporal frequency.

During the three days of temperature monitoring (implemented in late October 2018, just before groundwater recharge), some hydraulic changes in the borehole were clearly observed from the variation of flow rate at the top of the borehole that was increased by a factor of around two during the first night of monitoring. This hydraulic response could not be explained by tidal variations or atmospheric pressure changes but more likely due to water levels changes associated with the hydrological cycle and groundwater recharge. As we shall see in the following sections, these changes in flow rate were also associated with temperature variations in the borehole. In addition to the monitoring of natural hydraulic changes, a small pump (MP1- Grundfos) was installed in the first meters of the borehole at nearly the end (from 12:30 to 15:30 on the third day of the experiment) of the temperature monitoring period to increase the flow rate. This allows us to test the methodology used to monitor borehole flow changes in the borehole for three different conditions. Thus, throughout the monitoring period, the system was subjected to two different naturally occurring ambient conditions and one pumping condition (pumping flow rate around 40 l/min). For cross-validation of the flow profiles determined from temperature measurements, the flow has been also measured at different depths with a heat-Pulse Flowmeter (HPFM, Geovista) (Le Borgne et al., 2006) to well capture the flow variations along the borehole. HPFM is composed of an electrical resistance acting as a heat generator and two thermistors below and above the resistance. A heat-pulse is generated by the resistance and the travel time of the thermal breakthrough peak is recorded by one of the thermistors. The measured travel time is inversely proportional to the flow and the localization of the thermistor measuring the plume gives the direction of the flow. Note that a calibration process is used and described in the following to estimate the flow rate from travel time measurements. For each point measured by HPFM, we record the travel time at least three times to be able to quantify the uncertainty associated with the HPFM measurement. The mean standard deviation for travel time for ambient 1, ambient 2 and pumping hydraulic conditions are 1.92, 0.73 and 0.17 seconds corresponding to mean uncertainty of 1.1 lit/min, 2.45 lit/min and 2.92 lit/min. This mean uncertainty in flow measurement (dF) is obtained by taking the differential of both sides in the fitting equation (Figure S5 in supplementary materials) and using the mean uncertainty in the measured travel time as the uncertainty (dt) in travel time estimation. However, the uncertainty of the measurements is also defined locally at each point. The mean, and standard deviation of recorded travel times (at each point) are used to find the average flow rate and corresponding uncertainty.

4.2 Data Processing

4.2.1 FO-DTS calibration and processing

The conversion of the laser backscattered signal to temperature was done directly by the DTS unit using the double-ended calibration procedure (Van De Giesen et al., 2012). Due to the double-ended configuration, four coil sections of FO were installed before and after entering the borehole, in two baths filled with water at ambient temperature (15°C) and with wetted ice (0°C). To assess the accuracy and resolution of the temperature data recorded by DTS, few RBR temperature sensors with a temperature accuracy of 0.002 °C were also used in different locations, including the calibration baths (cold and ambient baths). One additional RBR solo T was set up to the top of the borehole in the water to check the calibration. A comparison of the temperature data recorded by DTS and RBRs reveals that the mean absolute error is around 0.05 °C and the maximum error was found to be 0.1 °C by DTS. Recorded temperature data normally inherits noises. Removing the noise from the data is essential for a successful interpretation and flow. Temperature inflection points, which may represent the entry of the fluid and consequently defining the production zones should not be indeed mistaken with local noise in the temperature at that location.

Smoothing was performed on time and not on space as details on the temperature variations in space are used for detection of the possible fracture locations. The locally Weighted Smoothing (LOESS) method (Cleveland, 1979) has been chosen to perform smoothing the data. LOESS uses locally weighted linear regression to smooth the data. It is weighted in the sense that a weighted function is defined within a span (window). Then a smoothed curve is obtained through a set of data defined by this dynamic span. The choice for value of span is critical to make sure that smoothing is effective and over-averaging will not happen which may result in losing resolution and dilution of the information (Moreno et al., 2014). Considering and trying the different spanning value for the smoothing process, we finally came up with a spanning of 10% of data. This means that moving smoothing window contain 10% (around 5 hours of recorded temperature data) of all observed temperature, each time it performs smoothing.

4.2.2 heat-pulse flowmeter calibration

Parallel to the recording of distributed temperature data, heat-pulse flow metering was performed in all three different flowing condition periods. For all tested points (depths) in the borehole, at least three measurements were done to reduce the measurement uncertainty following the methodology proposed by Paillet (1998). To calibrate heat-pulse data, we recorded the travel time just above all fractures and below the casing in the upper meters of the borehole, where the flow rate is maximum. At this location, the borehole wall is relatively smooth, and measurements were made for different pumping flow rates that were precisely measured from the timing to fill a large bucket (Figure S5 in the supplementary materials). The calibration has been used to convert travel times to flow rate assuming that borehole diameter is constant all along the borehole.

5. Field application

In this section, we first describe and analyze the spatio-temporal temperature data acquired in the borehole PZ-26. Then we show flow profile estimated by temperature data and compare it with velocity profile from HPFM.

5.1 Spatio-temporal temperature variations

Figure 5 shows the spatio-temporal temperature data acquired in 3 days of temperature monitoring at fractured borehole PZ-26. Three distinctive temperature patterns corresponding to three different hydraulic conditions can be clearly identified. The three different hydraulic conditions are shown by blue rectangle and labeled as Ambient1, Ambient 2 and pumping associated with three different flowrates measured at surface, 7 lit/min, 15.7 lit/min and 40 lit/min, respectively.

The temperature variations with time observed at a given depth corresponds to change of hydraulic conditions (ambient 1, ambient 2, and pumping). For instance, consider the yellow isotherm corresponding to the temperature of 15.1°C. It can be seen that this isotherm in ambient 1 condition reaches the depth of 70 m while in ambient 2 and pumping conditions in which flow rates are higher respectively, this isotherm is observed at 60 m and 20m respectively. This means that as the fluid velocity increases, the fluid retains its energy more as it has less time to exchange heat with surrounding media. Furthermore, in front of fracture at 75m, a green horizontal line in ambient 1, and a yellow horizontal line in ambient 2 and pumping conditions can be observed. This suggests a cold water inflow into the borehole. Similar inflows can be observed for fractures at 29 and 95 meters although temperature contrasts seem weaker. The locations of fractures are shown on the depth axis and it can be observed that many fracture locations correspond to temperature variations of the fluid.

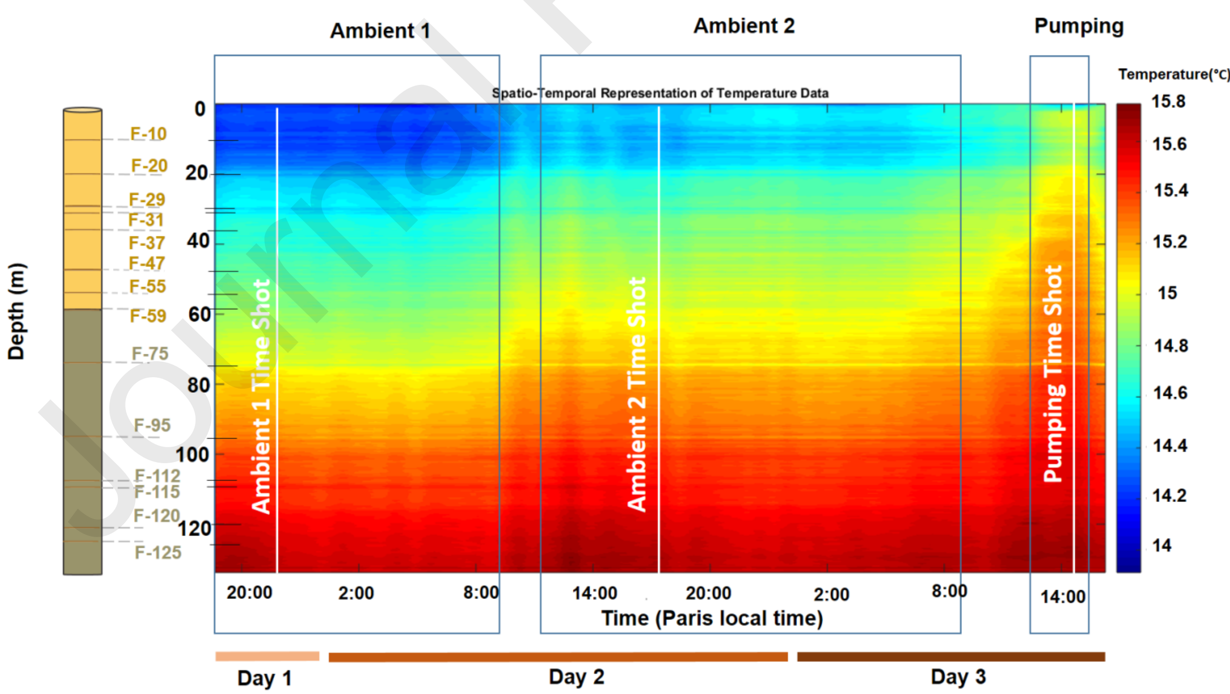

Figure 5: Representation of borehole schematic (left) with the position of the different fractures identified and Spatio-temporal temperature data (smoothed) recorded in borehole PZ-26 during the three different hydraulic conditions. The

bottom horizontal scale gives the timing of different events (ambient 1, ambient 2 and pumping). The temperature scale is provided on the right of the figure. The time range corresponding to approximately each event is presented by a blue rectangle. The white vertical lines correspond to the three-time shots chosen for temperature data to represent the three different hydraulic conditions. These time shots from smoothed temperature data then were used for vertical flow profiling.

The great advantage of FO-DTS is to provide full temporal monitoring that allows us to easily define some representative times of the different hydraulic conditions encountered. Thus, three-time shots from the DTS data representing three different flowing conditions (hydraulic conditions) were chosen to perform flow profiling in the borehole. These three-time shots are represented by vertical white lines in Figure 5. Because heat-pulse flow metering normally lasts a few hours, the time shots were chosen to be in the middle of the heat-pulse flow metering operation and ensuing these time shots lies within a stable temperature period. This results in a fair comparison between results obtained by heat-pulse flow metering and flow profiling done by using DTS data (The temperature profile is chosen from smoothed data). Figure 6 shows the three-time shots chosen for flow profiling (distributed temperature with depth). The blue, red and yellow curves represent ambient 1, ambient 2, and pumping conditions, respectively. It can be seen that increasing the flow rate results in less changes of temperature with depth. This happens because, for a fixed borehole length, higher the fluid velocity (rate), there will be less residence time for the fluid to do the heat exchange with the surrounding rock. This can be also seen in Figure 5 when comparing the same color spectrum for different depths. For example, the isotherm of red color in ambient 1 is in lower depth rather than ambient 2 and finally pumping condition. This means in the pumping, the fluid has conserved more of its energy compared to two other conditions. It is important to mention that prior knowledge of the locations of the fractures is essential for the interpretation of the temperature profile. However, in the case of no previous knowledge, finding the locations on the temperature profile where there is a heating (water coming to the borehole is colder with respect to the fluid in the borehole) or cooling (water coming to the borehole is hotter with respect to the fluid in the borehole) peak allow to infer the possible locations of the inflows. It must be noted that noise can create the same peaks but they are not stable with time while peaks corresponding to fluid inflows (with different temperatures) should persist at all times. It is worth mentioning that we see a sharp decrease in flowing water temperature at around 20m which is possibly due to introduction of cold surface water.

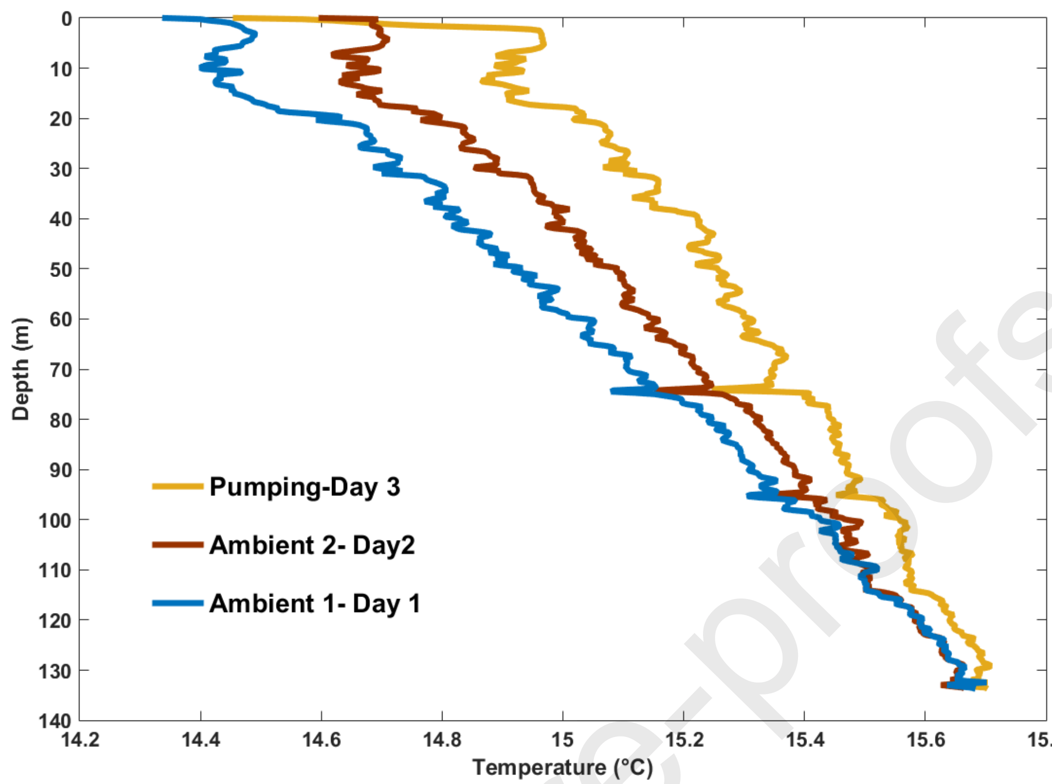

Figure 6: Comparison of three time-shots recorded temperature profile (smoothed) corresponding to the 3 different flowing conditions (ambient 1, ambient 2 and pumping).

5.2 Flow Rate calculations

Flow profiling using temperature data is quite dependent on proper knowledge of media thermal parameters as well as the flow history of the well (how flow rate varies with time which is used to calculate the flow time). In general, flow changes over time are not considered and media thermal properties are chosen at "known" constants. We implemented a full sensitivity analysis that is described in section 6. Here, we present and compare flow results obtained (1) by using the parameters suggested by Klepikova et al., (2011), who also did measurements/estimations of thermal parameters on the same site and (2) results obtained using the optimum values found by matching the manually measured surface flow rate to surface flow rates predicted by DTS (see section 6.1). However, it should be noted that these values may not necessarily represent realistic parameter values but mostly parameters obtained by tuning of surface flow rate predictions to surface flow rate measurements. These parameter values will be discussed in section 6. Although the parameter sensitivity will be discussed in section 6, this provides an idea of the sensitivity of the results depending on the parameters chosen. All parameter values used for flow rate estimations are given in table 1. The explanation of used parameters is also given in section 6.1.

Table 1: Fluid and Media Properties Used for Flow Profiling

Density of the rock (kg/m3)	Heat capacity of the rock (J/kg×°C)	Thermal conductivity of the fluid (W/m×°C)	Heat capacity of water (J/kg×°C)	Thermal diffusivity of the fluid (m2/s)	Rock thermal conductivity (W/m×°C)		Geothermal gradient (deg°C/m)		Flow time (day) for ambient1, ambient2, pumping (respectively)	
					Optimum value	Klepikova et al. (2011)	Optimum value	Klepikova et al. (2011)	Optimum value	Klepikova et al. (2011)
2560	790	0.59	4190	1.41 E-7	5.8	2.4	0.013	0.016	7,7,5	6,3,1

5.2.1 Flow Profiling using Distributed Temperature Sensing (DTS) Data

Recorded temperature data along with previously mentioned values for fluid and media properties are used to find the flow rate in different sections of the borehole. During ambient 1 condition, major active flowing fractures that are identified are fractures below 115m, 115m, 95m, and 55m and 35 m (Figure 7a). Figure 7, shows the locations of the main fractures, that are taken from the study by Bochet et al. (2020), by the horizontal dashed lines. It should be noted that fracture at 75m is contributing to the total flow with the entry of fluid with notably different temperatures as it can be seen in Figure 5. But its flow contribution is small and integrated with the fracture at 55m. The manually measured surface rate is around 7 l/min. The value of the estimated or measured flow rate from each fracture is shown in Figure 7(a) and quantified in table 2.

Ambient 2 condition occurred on the second day of the experiment as it was also observed at the site where the surface flow rate increased significantly. The measured surface flow rate is about 15.7 l/min. The analysis shows that major active flowing fractures are fractures below 115m, and fractures at 115m, 95m, 75m, 55m, and 35 m. The estimated individual contributions to the total flow are given in table 2. The value of the flow rate from each fracture is shown in Figure 7(b). Note that the two main contributing fractures seem to be the fracture at 35 and 55 meters deep.

Pumping started at noon of the third day (from 12:30 to 15:30) with rate of 40 lit/min. Pumping continued for three hours to let the fluid temperature stabilize in the borehole by extracting the fluid that already existed in the borehole. In Figure 5, it seems that except at the very early times, temperature during the pumping period is almost stable which was also a criterion to choose a proper time shot for the pumping period. Major active fractures, discerned by DTS are fractures below 115m, and at 115m, 95m, 75 and 55m and 35m. The value of the flow rate from each fracture can be observed in Figure 7(c) and is given in table 2. Note that, fractures at 95 and 115 m are the most productive fractures in that case.

Note that the uncertainty associated with estimation of borehole flows using DTS data stems from the uncertainty in the thermal parameters chosen. Defining a probable range of thermal parameters results in an uncertainty of the flow estimated.

5.2.2 Flow Profiling using Heat Pulse Flow meter (HPFM)

Heat-pulse flow metering in ambient 1 flowing condition was performed for a total of 12 points up to the depth of 62 m. It was not possible to do deeper measurements as the flow was too small, resulting in high variability of the recorded travel time with a large increase in the uncertainty of flow rate. Based on the analysis and interpretation of recorded travel time, fractures below 60m, 55m, and 35 m contribute to the total flow. Figure 7(a) compares the cumulative flow rate estimated by DTS data and heat-pulse flow meter with their associated error levels. Considering uncertainties of both measurements, it seems that both estimates agree fairly well. The cumulative flow rate measured by HPFM is 4.28 l/min for flow below F-55 and also fractures below F-115. Fracture contributions estimated both from DTS and HPFM are given in table 2 for comparison.

In ambient 2, a total of 10 measurement points was acquired up to the measured depth of 118m. Based on the analysis and interpretation of recorded travel times, fractures below 115m, and fractures at 115m, 95m, 55m, and 35 m contribute to the total flow. Figure 7(b) compares the cumulative flow rate estimated by DTS data and heat-pulse flow meter. Considering uncertainties, both estimates agree fairly well also in that case. The measured flow rate is shown and compared in table 2.

During pumping, a total of 9 points were acquired up to the measured depth of 118m. Based on the analysis and interpretation of recorded travel times, fractures below 115m, and fractures at 115m, 95m, 75m, 55m, 35 m, 20m, and 12 m contribute to the total measurable flow. Figure 7(c) compares the cumulative flow rate estimated by DTS data and heat-pulse flow meter. It is interesting to note that fracture at 55 (F-55) which was one the major producing fractures in ambient conditions, experiences a decrease in contribution during the pumping. This point will be discussed in the next section. It must be noted that in this case, the discrepancy between flow rate estimated by DTS and HPFM flow rate estimation can be mainly attributed to the fact that the selected flowing zone for interpretation of DTS data may not have been well established. Due to the increased velocity of the fluid in pumping, the distance required by the fluid to be traveled to establish a reliable flowing zone is longer and disturbed by the introduction of fluid into the borehole by other active fractures. It can also be observed that DTS cannot predict the rate in regions where the flowing zone is not established due to the high density of permeable fractures or inflows i.e. regions above 30 m. The measured flow rate is shown in Figure 7(c) and compared in table 2. Although more discrepancies may be observed in that case, flow rate estimates from DTS data agree relatively well with HPFM measurements.

Table 2: Contribution of each fracture to the total flow during ambient 1, ambient 2 and pumping conditions estimated from DTS data and measured by HPFM (note that for ambient 1 condition, F-55 and F-75 are merged together). As explained in the text, flow rates estimated from DTS data are calculated by using (1) the parameters suggested by Klepikova et al., (2011), and (2) the optimum values found by matching the manually measured surface flow rate to surface flow rates predicted by DTS (see section 6.1 and estimated parameters columns in the table below).

	Ambient 1	**Ambient 2**	**pumping**

Fractures	Estimated flow rate from DTS data		Measured flow rate from HPFM	Estimated flow rate from DTS data		Measured flow rate from HPFM	Estimated flow rate from DTS data		Measured flow rate from HPFM
	Using estimated parameters	Using Klepikova et al. (2011) parameters		Using estimated parameters	Using Klepikova et al. (2011) parameters		Using estimated parameters	Using Klepikova et al. (2011) parameters	
F-37 and above	1.8 l/min (25%)	1.7 l/min (24%)	1.58 l/min (22%)	4.12 l/min (27%)	5 l/min (33%)	3.38 lit/min (21.5%)	6.5 lit/min (17%)	8 lit/min (19%)	6.4 lit/min (17.5%)
F-55	1.4 l/min (19%)	1.4 l/min (20%)	1.51 l/min (20%)	3.9 l/min (25%)	3.9 l/min (25%)	3.5 l/min (22.5%)	0.5 lit/min (1.2%)	1.3 lit/min (3%)	0.8 l/min (2%)
F-75			4.28 l/min (58%)	1 l/min (6 %)	0.8 l/min (5%)	1.52 l/min (10%)	1 l/min (8 %)	2 lit/min (5%)	1.5 l/min (4%)
F-95	1.54 l/min (20%)	1.7 l/min (24%)		2.92 l/min (19 %)	2.6 l/min (17%)	2.46 l/min (16%)	13.35 lit/min (35%)	14.5 lit/min (35%)	9.5 l/min (24.5%)
F-115	1.9 l/min (26%)	1.7 l/min (24%)		2.93 l/min (19%)	2.35 l/min (15%)	1 l/min (6%)	12.25 lit/min (32%)	11.1 lit/min (26.5%)	10.6 l/min (27%)
Below F-115	0.7 l/min (10%)	0.5 l/min (8%)		0.62 l/min (4%)	0.65 l/min (5%)	3.68 l/min (23.4%)	5.25 lit/min (13.5%)	4.7 lit/min (11.5%)	9.6 lit/min (25%)

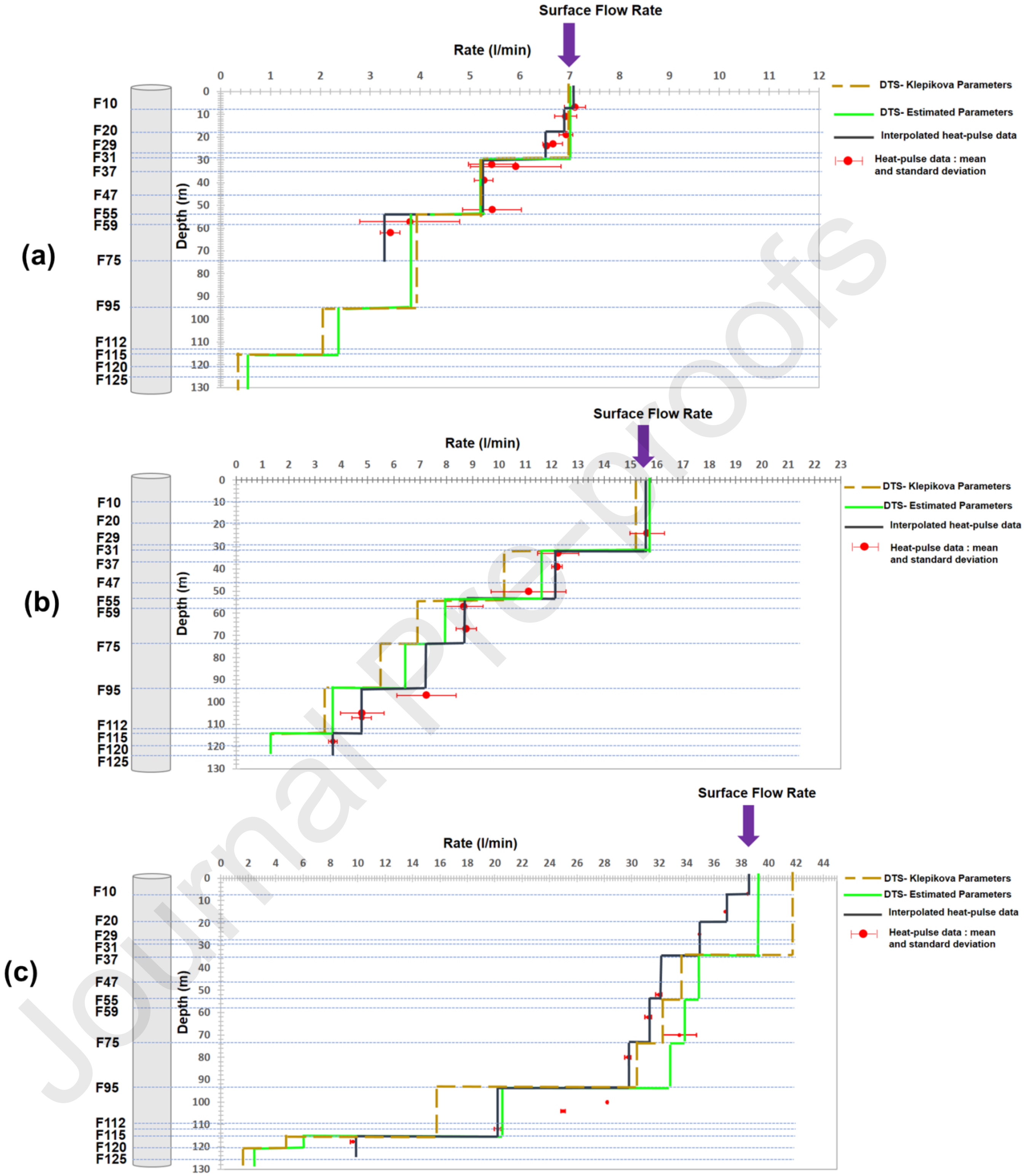

Figure 7- Comparison of flow rates estimated at different depth through DTS measurements and from HPFM measurements during ambient 1 (a), ambient 2 (b) and pumping (c) conditions. Green solid line shows flow profiles obtained by using estimated parameters from a sensitivity analysis (table 1) while brown dashed line shows flow profiles using Klepikova et al. (2011) parameters. Red dots show the measured flow rates by HPFM and their associated uncertainty in the measurement

Analysis of DTS data for flow profiling along with heat-pulse flow metering, show that there is a general agreement between flow measurements by HPFM and flows inferred from DTS data. Comparing two ambient conditions, we see the high flow variations on a daily basis which depend on different hydraulic conditions that are imposed on the system. During ambient conditions, half of the flows (56% in ambient 1 and 42% in ambient 2) are coming from the deep fractures (F-95 and below) and the other half coming from fractures above F-95. However, during the pumping, more than half of the flows (around 75%) is supplied from deep fractures (F-95 and below) and the rest is provided by other fractures. This can be also seen in Figure 6 as the bottom-hole temperature has shifted a little bit toward higher values during pumping which implies that water is provided from deeper depth. As we will address this point in the discussion, this is important as it gives an insight into the behavior of the system during ambient and pumping conditions since surface water and deep water contain different amounts of oxygen which may explain the essence of reactions that may happen in the borehole.

6. Discussion

In this section, we first describe the effect of thermal properties which are often unknown on the flow rate estimation. We then explain how it may be estimated for the purpose of flow profile measurement. Then we discuss the added values and drawbacks of using DTS in the field, in particular for monitoring groundwater dynamics.

6.1 Thermal parameters estimation

In order to perform successful flow profiling from temperature data, an estimate of the thermal properties values as well as the flow time is required. In this subsection, we describe the cases (i) when we know the thermal properties but flow time is unknown and (ii) when thermal properties and flow time are all unknown. We estimate the unknown properties by using a measured flow rate at the surface which permits constraining the estimated flow at the surface and therefore the unknown properties from the available temperature data.

In case that we have previous knowledge of geothermal gradient and rock thermal conductivity, we need to know the flow time to perform flow profiling from the temperature data. The flow time takes into the account, superposition of antecedent conditions. However, for a continuously flowing system with a daily variable flow rate, if the history of the flow is not recorded, then it is not straightforward to suggest a time and it can be used as a tuning parameter by matching the measured surface flow to estimated surface flow. In the present case, Klepikova et al., (2011) have reported values of 0.016 °C/m and 2.4 W/m×°C for geothermal gradient and rock thermal conductivity, for the same site. However, the value of flow time (which is required for the flow profiling) is unknown. To solve this issue, we determine the optimum flow time for each flowing condition, using the aforementioned thermal properties values and other required parameters (table 1) by matching the estimated surface flow rate by DTS and measured surface rate. In fact, here the flow time is used as a tuning parameter. The optimum flow times for ambient 1, ambient 2, and pumping conditions obtained are respectively 6 days, 3 days, and 1 day. This means that for ambient 1 condition, in order to reach the current thermal condition (to observe the same temperature trend in fluid along the borehole), it is needed to have a continuous flow of 7 lit/min (ambient 1) for 6 days. These individual flow times can be seen as a tuning parameter to calculate the flow rate. The results of using these parameters for flow profiling are presented in table 2 and Figure 7 and corresponds to the columns "using Klepikova et al. (2011), parameters.

However, in the case of no previous knowledge on thermal properties of the media as well as the flow time, we may estimate them all by matching the DTS-predicted surface flow rate and measured flow rate (flow rate at the surface) for all flowing conditions (ambient 1, ambient 2 and pumping). For doing so, we considered a uniform distribution for the geothermal gradient (0.01 to 0.03 deg°C/m), the rock thermal conductivity (2 to 6 W/m×°C), and the flow time (1 day to 365 days). The obtained optimum parameters for geothermal gradient and rock thermal conductivity are 0.013 (°C /m), 5.8 (W/m×°C), respectively. Consequently, the optimum flow time for ambient 1, ambient 2, and pumping are 7 days, 7 days, and 5 days. The results of flow estimated using these sets of parameters are given in table 2 and Figure 7 ("estimated parameters"). It must be noted that these estimated values may not necessarily reflect the real values but they can be used for estimation of flow from temperature data within a satisfactory range of error. It worth noting that Klepikova (2013) has reported values of thermal conductivities ranging from 1.731 (W/m×°C) to 3.42 (W/m×°C) for the mica-schist and 2.98 (W/m×°C) to 4.061 (W/m×°C) for the granite measured in the lab for rocks from the same geological site.

To discuss in more details, the effect of the choice of the different parameters, Figure 8 presents results obtained using two values of flow time (1 day and 182 days) on the range of optimum thermal property values. Every point in this Figure shows the average normalized error (with respect to standard deviation) of estimated surface flow by temperature data using corresponding geothermal gradient (on the x-axis) and thermal conductivity (on the y-axis) for 1 day and 182 days flow time. The dark blue region shows the range of values for a set of geothermal gradient and rock thermal conductivity with minimum error.

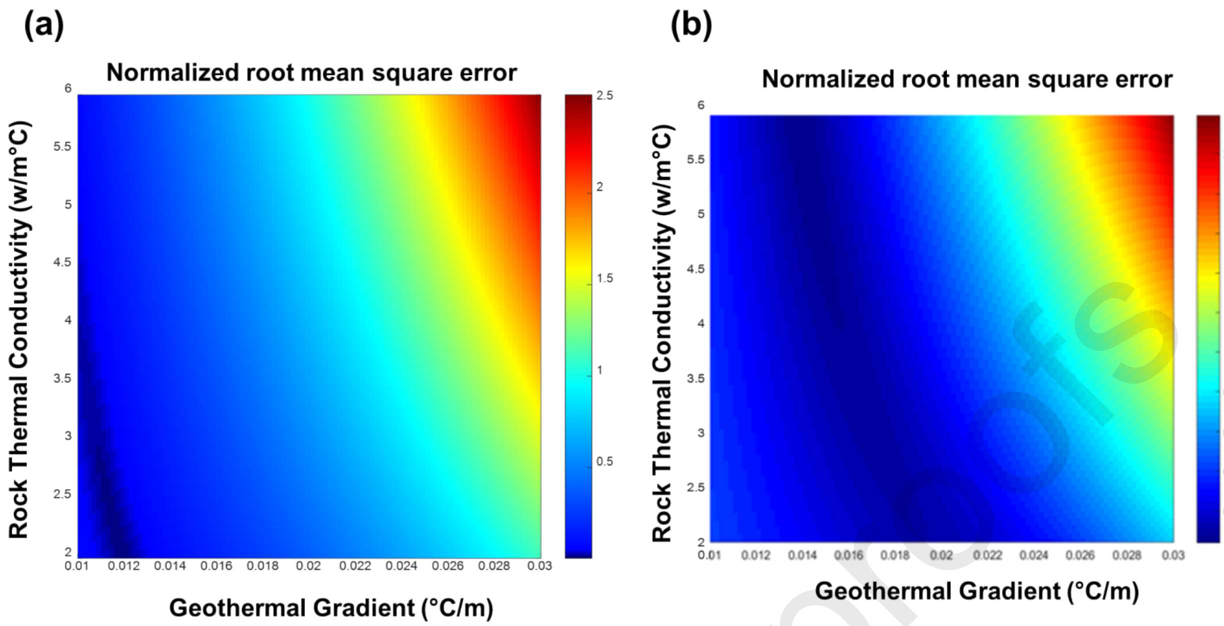

Figure 8: Normalized RMSE error between predicted flow by DTS and measured flow rate at the surface at (a) one-day flow time (b) six-months flow time

Based on Figure 8, it can be seen that the estimated flow rate is clearly more sensitive to the geothermal gradient rather than rock thermal conductivity (considering a fixed flow time). This has been also confirmed by the global sensitivity analysis performed in section 2.5. Secondly, it shows that for two different flow times, there are sets of thermal parameters that can result in the same small estimation errors regardless of the fact that whether they present real values or not. It must be noted that as long as the purpose of thermal parameter and flow time estimation is flow profiling, regardless of their values (whether they present real values or not), they can be used for estimation of flow from the temperature data. This would be an issue if the analysis was to be used to determine either thermal gradient or conductivity but since that is not the goal, then not knowing them exactly is not crucial. This is reflected in table 2 and Figure 7 as we used two sets of different parameters (Klepikova and optimized set of parameters) and we end up with a close estimation of the flow (by two sets of parameters) from the temperature data to the flow measured by HPFM.

6.2 Added values and drawbacks of using FO-DTS for field applications

In the classical approaches, the temperature sensors are used to record the temperature profile by pulling in and out the temperature probes or by recording the temperature in a fixed position with time. For instance, Klepikova et al. (2011; 2014) used temperature logging to infer the borehole flows with application to quantify inter borehole connectivity and fracture transmissivity. The use of FO-DTS has many advantages compared to classical probes. First, the introduction of DTS technology led to having both spatial and temporal information at the same time with data accessible during monitoring. This may be of great help for interpreting temperature signals during transient events or when groundwater dynamics cannot be fully understood by comparing simply two times shots. Moreover, using a

FO cable avoids fluid mixing in the borehole that can occur when logging the temperature probe. It also avoids generating head losses in the borehole, which may occur with the use of temperature probes or flowmeters. It is worth mentioning that when flow changes through time are expected, FO-DTS may be a complementary method.

There have been already previous attempts to use DTS for borehole flow profiling. For instance, Read et al. (2014) showed that the temperature difference between a heated cable and a non-heated cable can be used to quantify the vertical flows in the borehole like a distributed flowmeter. However, this approach may not be appropriate for long term monitoring as it requires more complex equipment to ensure continuous heating. Furthermore, the calibration of this method for low flow rate, in particular for ambient conditions, is challenging and uncertain (Read et al., 2014). Some other attempts like Leaf et al. (2012), Sellwood et al. (2015) and Read et al. (2015) used the injection of hot water or an electrical heater to infer water direction and velocities in the borehole in ambient and hydraulically stressed conditions. However, these methods provide more accurate results close to the heating source and were not used for continuous monitoring. More recently, Selker and Selker (2018) used a distributed borehole heater to investigate water movement within and near wells, but the methodology proposed requires specific heating cables. In comparison, our field installation just requires monitoring temperature with a DTS unit. Although field DTS units having low electrical consumptions are currently developed, this may still be the main limitation in some field cases. Nevertheless, using distributed temperature data is beneficial since it is easy to install in the field, it leads to a minimal disturbance of borehole natural conditions and provides real-time data acquisition.

6.3 Inferring groundwater dynamics from temperature data

In the present study, we proposed a simple approach based on an analytical model to infer borehole flows from temperature data. Using a numerical model for inversion of temperature data may be indeed computationally expensive for some models while here we have substituted it with very fast and reasonably accurate analytical solutions. In addition, using DTS data, we addressed the temporal changes in temperature and showed the potential of using these types of data for capturing the dynamic response of the fractured media. One main challenge associated with this approach is having proper knowledge of the media's thermal properties. However, we showed that measuring the surface flow rate in the case of an artesian borehole can be of great help to obtain the proper value of thermal properties for flow profiling by constraining the calculated flow to measured flow at the surface. Another limitation comes from the scale of observation which remains limited to the borehole scale. Nevertheless, we have shown in the previous section how FO-DTS can be used to infer flow variations and monitor the transient nature of the fracture system.

Once the flow from each fracture is estimated, it can be easily used to calculate the transmissivity of each fracture if the borehole transmissivity is known (Paillet, 1998; Day-Lewis et al., 2011). Considering the value of 5×10^{-3} m^2/s for the total transmissivity, that has been reported by Bochet et al. (2020) from a pumping test in the same borehole, the fractures transmissivities at different depths are estimated to vary between 10^{-4} and 1.7×10^{-3} m^2/s. Note that here, we observe roughly the same proportion of flow coming from the different fractures between ambient1 and ambient2 conditions. Nevertheless, in pumping conditions, the flow coming from the fracture at 55 meters is smaller than in ambient conditions. This is confirmed by the interpretation of DTS data and also by HPFM measurements which show that during pumping, the flow is produced mainly by fracture at 95 and 115m (Figure 7). This is quite surprising since the head in the borehole is lower for pumping conditions compared to ambient conditions and should therefore lead to an increase of flow coming from F-55. This suggests that the different inflows cannot be analyzed independently and that fracture F-55 is possibly somehow connected to complex fracture networks so that the inflow observed at 55 m in some conditions may be greatly dependent on the head distribution in the fracture network. This may have some implications when using classical borehole flowmetry to infer fracture transmissivity (Paillet, 1998; Day-Lewis et al., 2011). This may also explain some intermittent fluxes observed from fracture F-55, which provides at specific times, water enriched with Oxygen that is at the origin of bacterial development (Bochet et al., 2020). Long-term temperature monitoring may provide a better imaging of this intermittent behavior in groundwater dynamics. Note that the approach could be expanded to monitor the dynamic nature of recharge within the aquifer. It should be also noted that even though the experimental and numerical validation of the work is implemented in crystalline rock aquifers; there is no limiting assumption that would limit the application of the approach to other types of aquifers like sedimentary aquifers.

7. Conclusions

In the current work, DTS data were used to calculate flows in different sections of the borehole and consequently quantify the flow from each producing fracture during the different hydraulic conditions. To be able to use temperature data for real-time flow profiling, a computationally fast tool is proposed to transform temperature profile to flow profile. This tool employs an analytical solution by Hassan and Kabir (1994) and Ramey (1962) for flow profiling. Comparing the results obtained from heat-pulse flow metering and DTS shows that the framework can estimate the flow rate with a good accuracy where there is a well-established fluid temperature profile. Results confirm the general agreement between flow rates estimated by DTS and flow rates measured by HPFM. During ambient 1 and ambient 2 flowing conditions, it seems that the repetition of flow measurements along the borehole is different but difficult to catch with heat-pulse flow metering while DTS flow profiling can be very convenient and useful in ambient conditions. However, one of the challenges of using the current approach is the proper knowledge of the thermal properties of media required to infer the flow rate from the temperature. In case of a lack of knowledge of the media's thermal properties, surface rate measurement can be useful to constrain the model and reduce the flow profiling uncertainty.

The use FO-DTS data to monitor the dynamic behavior of a fractured system at the borehole scale has many advantages. It allowed us to capture changes in the flow inside the borehole once hydraulic conditions of the system changed naturally (from ambient 1 to ambient 2) and artificially (from ambient 2 to pumping). DTS data in PZ26 has many interesting aspects to note. Firstly, some fractures may be easily detected through temperature trace when there is a sufficient temperature contrast between the water exiting from the fracture and the water inside the borehole. Secondly, it shows its ability for monitoring daily borehole flow variations of flow at different temporal scales. Such a possibility opens a new window for real-time monitoring of complex fracture interactions and recharge processes in fractured media.

The advantage of the proposed method (DTS data and proposed framework) compared to conventional methods (such as heat-pulse flow meter) is that it requires less time and effort and it provides continuous monitoring appropriate for detecting rapid changes. Also, distributed sensors are made of FOs and due to their narrow diameters, they can be used where there is a risk or limitation with the utilization of other tools of larger diameters. Furthermore, another interesting aspect of the DTS is that it provides spatial and temporal temperature data which can be used to do real-time monitoring and understanding the change in the state of the system with time (monitoring the dynamics of the system). In the present case, results show that fractures contribution varies significantly depending on hydraulic conditions. Beyond the transient nature of this fractured aquifer, this has also some consequences on mixing and reactivity occurring inside the borehole. Indeed, some Oxygen rich fractures like the fracture at 55 meters deep, appear to be characterized by varying borehole inflows and possible intermittent fluxes which may be due to complex interactions with others fractures. By inferring borehole flow variations, temperature could be thus a possible proxy for characterizing mixing at the borehole scale.

CRediT authorship contribution statement

Pouladi, B.: Conceptualization, Methodology, computer code development, Investigation, Writing - original draft, editing. **Bour, O**.: Methodology, Investigation, Writing - review & editing, Supervision. **Longuevergne, L**.: Methodology, - review & editing, Supervision. **La Bernardie, J**.: Investigation, review & editing. **Simon, N**.: Investigation

Declaration of Competing Interest

The authors declare that they have no known competing financial interests or personal relationships that could have appeared to influence the work reported in this paper.

Acknowledgments

This project has received funding from the European Union's Horizon 2020 research and innovation program under the Marie Sklodowska-Curie Grant Agreement No 722028 (ITN project ENIGMA). This work is also part of the ANR project EQUIPEX CRITEX (grant ANR-11-EQPX-0011) from which we received financial support. We thank very much the SNO H+ (Réseau National de sites Hydrogéologiques) for field and technical support.

The data presented in this paper are available and accessible through the following link at the database of the French National Network for Hydrogeological sites:

(http://hplus.ore.fr/en/pouladi-et-al-2021-joh-data).

The computer code will be also available upon request to any of the authors.

Appendix A – Heat Transfer Model

Let's consider a control volume inside the borehole spanning from the depth z to z-dz (Figure 1), assuming that we have steady-state heat transfer inside the wellbore and transient heat transfer to the formation, energy balance for wellbore is written as follow:

[energy entering the control volume] = [energy out of the control volume]

$$[(wH)_z-(wH)_{z-dz}]+\frac{1}{2}[(wv^2)_z-(wv^2)_{z-dz}]+[z(wg)_z-(z-dz)(wg)_{z-dz}]=Qdz \quad \text{(A-1)}$$

Dividing by dz and w, then evaluating the expression as $\lim_{dz\to 0}$, we have,

$$\frac{dH}{dz}+v\frac{dv}{dz}-g=\frac{Q}{w} \quad \text{(A-2)}$$

Where H, g , v, Q and w are enthalpy of the fluid, gravity acceleration, fluid velocity, heat transfer from the fluid to surrounding media and fluid mass rate, respectively. The above equation states that change in Enthalpy of the fluid in the wellbore plus fluid gravitational and kinetic energy terms equal to heat transfer between the fluid and surrounding area per unit of the flowing fluid mass. Assuming that no phase change occurs in the fluid, enthalpy can be written as the following form in terms of measurable parameters, fluid's Temperature (T_f), and Pressure (p).

$$dH=\left(\frac{\partial H}{\partial T_f}\right)_P dT_f+\left(\frac{\partial H}{\partial p}\right)_T dp=C_p dT_f-C_J C_p dp \quad \text{(A-3)}$$

where Cp and CJ are Specific Heat Capacity of Water and Joule-Thompson coefficient. Specific heat capacity defines the amount of energy required for a unit to increase the temperature of the water. Joule-Thompson coefficient defines the change in the temperature of fluid when it is subjected to the pressure change process. It can be a positive value (mostly for gases at moderate pressure), resulting in temperature drop or negative values (mostly for liquids) and resulting in temperature increase.

Using equation (3) in equation (2) and rearranging the terms, the following form is obtained:

$$\frac{dT_f}{dZ}=C_J\frac{dp}{dz}+\frac{1}{C_P}[\frac{Q}{W}+g-v\frac{dv}{dz}] \quad \text{(A-4)}$$

Writing up the energy balance for the formation leads to the following equation:

$$\frac{\partial^2 T_e}{\partial r^2}+\frac{1}{r}\frac{\partial T_e}{\partial r}=\frac{c_e \rho_e}{k_e}\frac{\partial T_e}{\partial t} \tag{A-5}$$

Where Te, Ce, ρe and ke are rock temperature, rock heat capacity, rock density, and rock thermal conductivity, respectively.

Different methods and solutions are proposed by authors to solve the aforementioned equations. These solutions are based on some assumptions on the real physics of the problem. One of the most critical ones is the boundary condition between the wellbore and the surrounding earth. Authors have considered constant heat flux or constant temperature boundary conditions at the wellbore/earth interface while none of them generally explains the heat transfer problem as neither heat flux condition nor constant temperature condition remain constant (Satman and Tureyen, 2016). However, both solutions converge at long times. The other assumption is about the borehole. Ramey has considered the borehole as a line source while Hasan and Kabir have considered a finite radius for the borehole. Ramey's solution is most suitable for cases when conduction becomes the main heat loss mechanism which happens in low flow conditions. It has been reported that Ramey's solution is accurate except in early times (Hagoort, 2004) when heat flow in the wellbore is controlled by convection, and when the assumed conditions are not met. The Ramey and Hasan and Kabir solutions are given in equations (A-6) to (A-10) respectively.

$$T_f=T_{ei}+\frac{[1\text{-}e^{(z-z_j)L_r}]}{L_r}(GG\text{-}\frac{g}{c_p})+[T_{fj}\text{-}T_{eij}]e^{(z-z_j)L_r} \tag{A-6}$$

$$L_r{}^{Ramey}=\frac{wc_p f(t_d)}{2\pi k_e} \tag{A-7}$$

$$t_d=\frac{k_e t}{r_{wb}{}^2} \tag{A-8}$$

$$f\,(t_d)=\ln(\frac{2\sqrt{k_e t_d}}{r_w})\text{-}0.29 \tag{A-9}$$

$$L_r{}^{Hassan\ \&\ Kabir}=\frac{c_p w}{2\pi}[\frac{k_e+r_{wb}U_t f\,(t_d)}{r_{wb}U_t k_e}] \tag{A-10}$$

Here A is called relaxation distance. This is the length required by the fluid to be traveled so as the fluid temperature becomes parallel to the geothermal temperature. A dimensionless time function $f(t_d)$ is introduced, accounting for change of heat transfer coefficient with time. Various forms of time functions existing in the literature have been studied and compared by Satman and Tureyen (2016). They suggested that dimensionless time function by Kutun et al. (2014) as given in equations (11) and (12), would be sufficiently accurate for engineering purposes for all values of heat flow time. Other terms used in the above equations are given in nomenclature.

References

Alemán, D.I.O., 2018. Fracture Flow Rate Estimation Using Machine Learning On Temperature Data (Doctoral dissertation, Stanford University).

Anderson, M.P., 2005. Heat as a groundwater tracer. Groundwater, 43(6): 951-968.

Berkowitz, B., 2002. Characterizing flow and transport in fractured geological media: A review. Advances in water resources, 25(8-12), pp.861-884.

Bochet, O., 2017. Caractérisation des hot spots de réactivité biogéochimique dans les eaux souterraines (Doctoral dissertation, Université Rennes 1).

Bochet, O., L. Bethencourt, A., Dufresne, J., Farasin, M., Pédrot, T., Labasque, E., Chatton, N., Lavenant, C., Petton, B.W., Abbott, L., Aquilina, and T. Le Borgne, 2020. Iron-oxidizer hotspots formed by intermittent oxic–anoxic fluid mixing in fractured rocks, Nature Geoscience 13(2), pp. 149-155

Chatelier, M., Ruelleu, S., Bour, O., Porel, G. and Delay, F., 2011. Combined fluid temperature and flow logging for the characterization of hydraulic structure in a fractured karst aquifer. Journal of Hydrology, 400(3-4), pp.377-386.

Coleman, T.I., Parker, B.L., Maldaner, C.H., Mondanos, M.J., 2015. Groundwater flow characterization in a fractured bedrock aquifer using active DTS tests in sealed boreholes. Journal of Hydrology, 528: 449-462.

Cleveland, W.S., 1979. Robust locally weighted regression and smoothing scatterplots. Journal of the American statistical association, 74(368), pp.829-836.

Comsol multiphysics® v. 5.4. (2018). COMSOL AB, Stockholm, Sweden. (from www.comsol.com)

Day-Lewis, F.D., Johnson, C.D., Paillet, F.L. and Halford, K.J., 2011. A computer program for flow-log analysis of single holes (FLASH). Groundwater, 49(6), pp.926-931.

Day-Lewis, F.D., Slater, L.D., Robinson, J., Johnson, C.D., Terry, N. and Werkema, D., 2017. An overview of geophysical technologies appropriate for characterization and monitoring at fractured-rock sites. Journal of environmental management, 204, pp.709-720.

de Dreuzy, Bodin, J., Le Grand, H., Davy, P., Boulanger D., Battais A., Bour O., Gouze P., Porel G., 2006. Groundwater database for site and processes studies : Point-like structure based on well, meteorological and hydrological platforms, *Groundwater,44*(5), pp 743-748.

Drost, W., Klotz, D., Koch, A., Moser, H., Neumaier, F. and Rauert, W., 1968. Point dilution methods of investigating ground water flow by means of radioisotopes. Water resources research, 4(1), pp.125-146.

Edwardson, M., Girner, H., Parkison, H., Williams, C., Matthews, C., 1962. Calculation of formation temperature disturbances caused by mud circulation. Journal of Petroleum Technology, 14(04): 416-426.

Gaillardet, J., Braud, I., Hankard, F., Anquetin, S., Bour, O., Dorfliger, N., De Dreuzy, J.R., Galle, S., Galy, C., Gogo, S. and Gourcy, L., 2018. OZCAR: The French network of critical zone observatories. Vadose Zone Journal, 17(1), pp.1-24.

Hagoort, J., 2004. Ramey's wellbore heat transmission revisited. SPE journal, 9(04): 465-474.

Hasan, A.R., Kabir, C., 1994. Aspects of wellbore heat transfer during two-phase flow (includes associated papers 30226 and 30970). SPE Production & Facilities, 9(03): 211-216.

Hasan, A.R., Kabir, C.S., 2007. A simple model for annular two-phase flow in wellbores, SPE Production & Operation. 22 (2): 168-175

Hasan, A.R., Kabir, C.S., Sarica, C., 2002. Fluid flow and heat transfer in wellbores. Society of Petroleum Engineers Richardson, TX. pp. 23-46

Hasan, A.R., Kabir, C.S., Wang, X., 2009. A robust steady-state model for flowing-fluid temperature in complex wells. SPE Production & Operations, 24(02): 269-276.

Hess, A.E., 1986. Identifying hydraulically conductive fractures with a slow-velocity borehole flowmeter. Canadian Geotechnical Journal, 23(1): 69-78.

Horne, R., Shinohara, K., 1979. Wellbore heat loss in production and injection wells. Journal of Petroleum Technology, 31(01): 116-118.

Hsieh, P.A., 1998. Scale Effects in Fluid Flow Through Fractured Geological Media, Scale Dependence and Scale Invariance in Hydrology. Cambridge University Press , pp. 335–353

Jamin, P., Goderniaux, P., Bour, O., Le Borgne, T., Englert, A., Longuevergne, L. and Brouyère, S., 2015. Contribution of the finite volume point dilution method for measurement of groundwater fluxes in a fractured aquifer. Journal of Contaminant Hydrology, 182, pp.244-255.

Jiménez-Martínez, J., Longuevergne, L., Le Borgne, T., Davy, P., Russian, A. and Bour, O., 2013. Temporal and spatial scaling of hydraulic response to recharge in fractured aquifers: Insights from a frequency domain analysis. Water Resources Research, 49(5), pp.3007-3023.

Kabir, C., Hasan, A., Jordan, D., Wang, X., 1996. A wellbore/reservoir simulator for testing gas wells in high-temperature reservoirs. SPE Formation Evaluation, 11(02): 128-134.

Kabir, C., Izgec, B., Hasan, A., Wang, X., 2012. Computing flow profiles and total flow rate with temperature surveys in gas wells. Journal of Natural Gas Science and Engineering, 4: 1-7.

Keys, W.S., 1990. Borehole geophysics applied to ground-water investigations (Vol. 6375). Dublin, Ohio: National Water Well Association.

Klepikova, M.V., T. Le Borgne, O. Bour and P. Davy, 2011. A methodology for using borehole temperature-depth profiles under ambient, single and cross-borehole pumping conditions to estimate fracture hydraulic properties, *Journal of Hydrology* 407, pp 145–152.

Klepikova, M., 2013. Imaging of fractured rock properties from flow and heat transport: field experiments and inverse modelling (Doctoral dissertation, Université Rennes 1).

Klepikova, M.V., T. Le Borgne, O. Bour, K. Gallagher, R. Hochreutener and N. Lavenant,., 2014. Passive temperature tomography experiments to characterize transmissivity and connectivity of preferential flow paths in fractured media. Journal of Hydrology, 512: 549-562.

Klotz, D., Seiler, K.P., Moser, H. and Neumaier, F., 1980. Dispersivity and velocity relationship from laboratory and field experiments. Journal of Hydrology, 45(3-4), pp.169-184.

Kluth, R., Naldrett, G., 2009. Fiber-optic DTS flow profiling installed in advanced MRC well. Journal of Petroleum Technology, 61(04): 30-32.

Kutun, K., Tureyen, O.I., Satman, A., 2014. Temperature behavior of geothermal wells during production, injection and shut-in operations, Proceedings, 39th Workshop on Geothermal Reservoir Engineering, Stanford University, Stanford, California, February, pp. 24-26.

Leaf, A. T., D. J. Hart, and J. M. Bahr (2012), Active thermal tracer tests for improved hydrostratigraphic characterization, Ground Water, 50(5), 726–735,

Le Borgne, T., Paillet, F., Bour, O., Caudal, J.P., 2006. Cross-borehole flowmeter tests for transient heads in heterogeneous aquifers. Groundwater, 44(3): 444-452.

Leray, S., De Dreuzy, J.R., Bour, O., Labasque, T. and Aquilina, L., 2012. Contribution of age data to the characterization of complex aquifers. Journal of Hydrology, 464, pp.54-68.

Lesem, L.B., Greytok, F., Marotta, F., McKetta Jr, J.J., 1957. A method of calculating the distribution of temperature in flowing gas wells. Transactions of the american institute of mining and metallurgical engineers. 210(6): 169-176

Luo, H., Li, H., Lu, Y., Li, Y. and Guo, Z., 2020. Inversion of distributed temperature measurements to interpret the flow profile for a multistage fractured horizontal well in low-permeability gas reservoir. Applied Mathematical Modelling, 77, pp.360-377.

Luo, H., Li, H., Tan, Y., Li, Y., Jiang, B., Lu, Y. and Cui, X., 2020. A novel inversion approach for fracture parameters and inflow rates diagnosis in multistage fractured horizontal wells. Journal of Petroleum Science and Engineering, 184, p.106585.

Maldaner, C.H., Munn, J.D., Coleman, T.I., Molson, J.W., Parker, B.L., 2019. Groundwater flow quantification in fractured rock boreholes using active distributed temperature sensing under natural gradient conditions. Water Resources Research. 55, 3285–3306.

Meyzonnat, G. et al., 2018. High-Resolution Wellbore Temperature Logging Combined with a Borehole-Scale Heat Budget: Conceptual and Analytical Approaches to Characterize Hydraulically Active Fractures and Groundwater Origin. Geofluids, 2018, 19.

Michalski, A., Klepp, G.M., 1990. Characterization of transmissive fractures by simple tracing of in-well flow. Groundwater, 28(2): 191-198.

Molz, F., Boman, G., Young, S., Waldrop, W., 1994. Borehole flowmeters: Field application and data analysis. Journal of Hydrology, 163(3-4): 347-371.

Moreno, Á., García-Haro, F.J., Martínez, B., Gilabert, M.A., 2014. Noise reduction and gap filling of fapar time series using an adapted local regression filter. Remote Sensing, 6(9): 8238-8260.

Moss, J., White, P., 1959. How to calculate temperature profiles in a water-injection well. Oil and Gas J, 57(11): 174.

Munn, J.D., Maldaner, C.H., Coleman, T.I. and Parker, B.L., 2020. Measuring fracture flow changes in a bedrock aquifer due to open hole and pumped conditions using Active Distributed Temperature Sensing. Water Resources Research, p.e2020WR027229.

Nian, Y.L. and Cheng, W.L., 2018. Insights into geothermal utilization of abandoned oil and gas wells. Renewable and Sustainable Energy Reviews, 87, pp.44-60..

Novakowski, K., Bickerton, G., Lapcevic, P., Voralek, J. and Ross, N., 2006. Measurements of groundwater velocity in discrete rock fractures. Journal of contaminant hydrology, 82(1-2), pp.44-60.

Nuñez-Lopez, V., Muñoz-Torres, J., Zeidouni, M., 2014. Temperature monitoring using distributed temperature sensing (DTS) technology. Energy Procedia, 63: 3984-3991.

Ouyang, L.-B., Belanger, D., 2004. Flow Profiling via Distributed Temperature Sensor (DTS) System-Expectation and Reality, SPE Prod &Oper 21 (1): 269-281. SPE-90541-PA.

Paillet, F.L., Hess, A., Cheng, C., Hardin, E., 1987. Characterization of fracture permeability with high-resolution vertical flow measurements during borehole pumping. Groundwater, 25(1): 28-40.

Paillet, F.L., 1998. Flow modeling and permeability estimation using borehole flow logs in heterogeneous fractured formations. Water Resources Research, 34(5), pp.997-1010.

Pehme, P.E., Parker, B.L., Cherry, J.A. and Greenhouse, J.P., 2010. Improved resolution of ambient flow through fractured rock with temperature logs. Groundwater, 48(2), pp.191-205.

Pianosi, F., Sarrazin, F., Wagener, T., 2015. A Matlab toolbox for global sensitivity analysis. Environmental Modelling & Software, 70: 80-85.

Pitrak, M., Mares, S. and Kobr, M., 2007. A simple borehole dilution technique in measuring horizontal ground water flow. Groundwater, 45(1), pp.89-92.

Preto, P., Stranne, C., Greenwood, S., Jakobsson, M., Näslund, J.O., Sundberg, J., Swärd, H. and O'Regan, M., 2019. Geothermal evidence for groundwater flow through Quaternary sediments overlying bedrock aquifers below Lake Vättern, Sweden. GFF, 141(2), pp.106-120.

Ramey Jr, H., 1962. Wellbore heat transmission. Transactions of the society of petroleum engineers, 225(04): 427-435, doi:10.2118/96-PA

Read T., Bour O., Bense V., Le Borgne T., Goderniaux P., Klepikova , M.V., Hochreutener R., Lavenant N., and Boschero V., 2013. Characterizing groundwater flow and heat transport in fractured rock using Fibre-Optic Distributed Temperature Sensing, *Geophysical Research Letters*, vol. 40 *(10)*, 2055–2059, doi:10.1002/grl.50397.

Read, T., O. Bour, J. S. Selker, V. F. Bense, T. Le Borgne, R. Hochreutener, and N. Lavenant, 2014. Active-distributed temperature sensing to continuously quantify vertical flow in boreholes. Water Resources Research, 50(5): 3706-3713.

Read T, Bense VF, Bour O, Le Borgne T, Lavenant N, Hochreutener R, Selker JS (2015) Thermal-plume fibre optic tracking (T-POT) test for flow velocity measurement in groundwater boreholes. Geoscientific Instrumentation, Methods and Data Systems Discussions 4, 197–202.

Roques, C., Bour, O., Aquilina, L., Dewandel, B., 2016. High-yielding aquifers in crystalline basement: insights about the role of fault zones, exemplified by Armorican Massif, France. Hydrogeology journal, 24(8): 2157-2170.

Roques C, Aquilina L., Boisson A., Vergnaud-Ayraud V., Labasque T., Longuevergne L., Laurencelle M., Dufresne A., de Dreuzy J.R, Pauwels H. and O. Bour, 2018. Autotrophic denitrification supported by biotite dissolution in crystalline aquifers: (2) transient mixing and denitrification dynamic during long-term pumping, *Science of the Total Environment 619–620*, 491–503.

Ruelleu, S. F. Moreau, O. Bour, D. Gapais and G. Martelet 2010. Impact of gently dipping discontinuities on basement aquifer recharge: An example from Ploemeur (Brittany, France), J of Applied Geophysics, V 70, N° 2, pp 161-168, doi10.1016/j.jappgeo.2009.12.007.

Sagar, R., Doty, D., Schmidt, Z., 1991. Predicting temperature profiles in a flowing well. SPE production engineering, 6(04): 441-448.

Satman, A., Tureyen, O.I., 2016. Geothermal wellbore heat transmission: Stabilization times for “static” and “transient” wellbore temperature profiles. Geothermics, 64: 482-489.

Satter, A., 1965. Heat losses during flow of steam down a wellbore. Journal of Petroleum technology, 17(07): 845-851.

Selker, F. and Selker, J.S., 2018. Investigating water movement within and near wells using active point heating and fiber optic distributed temperature sensing. Sensors, 18(4), p.1023.

Sellwood, S.M., Hart, D.J. and Bahr, J.M., 2015. An in-well heat-tracer-test method for evaluating borehole flow conditions. Hydrogeology Journal, 23(8), pp.1817-1830.

Silliman, S. and Robinson, R., 1989. Identifying fracture interconnections between boreholes using natural temperature profiling: I. Conceptual basis. Groundwater, 27(3), pp.393-402.

Silva, W.L., Lima, V.S., Fonseca, D.A., Salazar, A.O., Maitelli, C.W. and Echaiz E, G.A., 2019. Study of Flow Rate Measurements Derived from Temperature Profiles of an Emulated Well by a Laboratory Prototype. Sensors, 19(7), p.1498.

Song, X., Shi, Y., Li, G., Shen, Z., Hu, X., Lyu, Z., Zheng, R. and Wang, G., 2018. Numerical analysis of the heat production performance of a closed loop geothermal system. Renewable Energy, 120, pp.365-378.

Touchard, F., 1998. Caractérisation hydrogéologique d'un aquifère en socle fracturé: Site de Ploemeur (Morbihan) (Doctoral dissertation, Université Rennes 1).

Van De Giesen, N. et al., 2012. Double-ended calibration of fiber-optic Raman spectra distributed temperature sensing data. Sensors, 12(5): 5471-5485.

Vitale, S.A., Robbins, G.A., 2017. Measuring flow rate in crystalline bedrock wells using the dissolved oxygen alteration method. Groundwater, 55(4): 588-592.

Wang, Z., 2012. The uses of distributed temperature survey (DTS) data (Doctoral dissertation, Stanford University).

Wang, J., Nitschke, F., Korzani, M.G. and Kohl, T., 2019. Temperature log simulations in high-enthalpy boreholes. Geothermal Energy, 7(1), p.32..

CRediT authorship contribution statement

Pouladi, B.: Conceptualization, Methodology, computer code development, Investigation, Writing - original draft, editing. **Bour, O**.: Methodology, Investigation, Writing - review & editing, Supervision. **Longuevergne, L**.: Methodology, - review & editing, Supervision. **La Bernardie, J**.: Investigation, review & editing. **Simon, N**.: Investigation

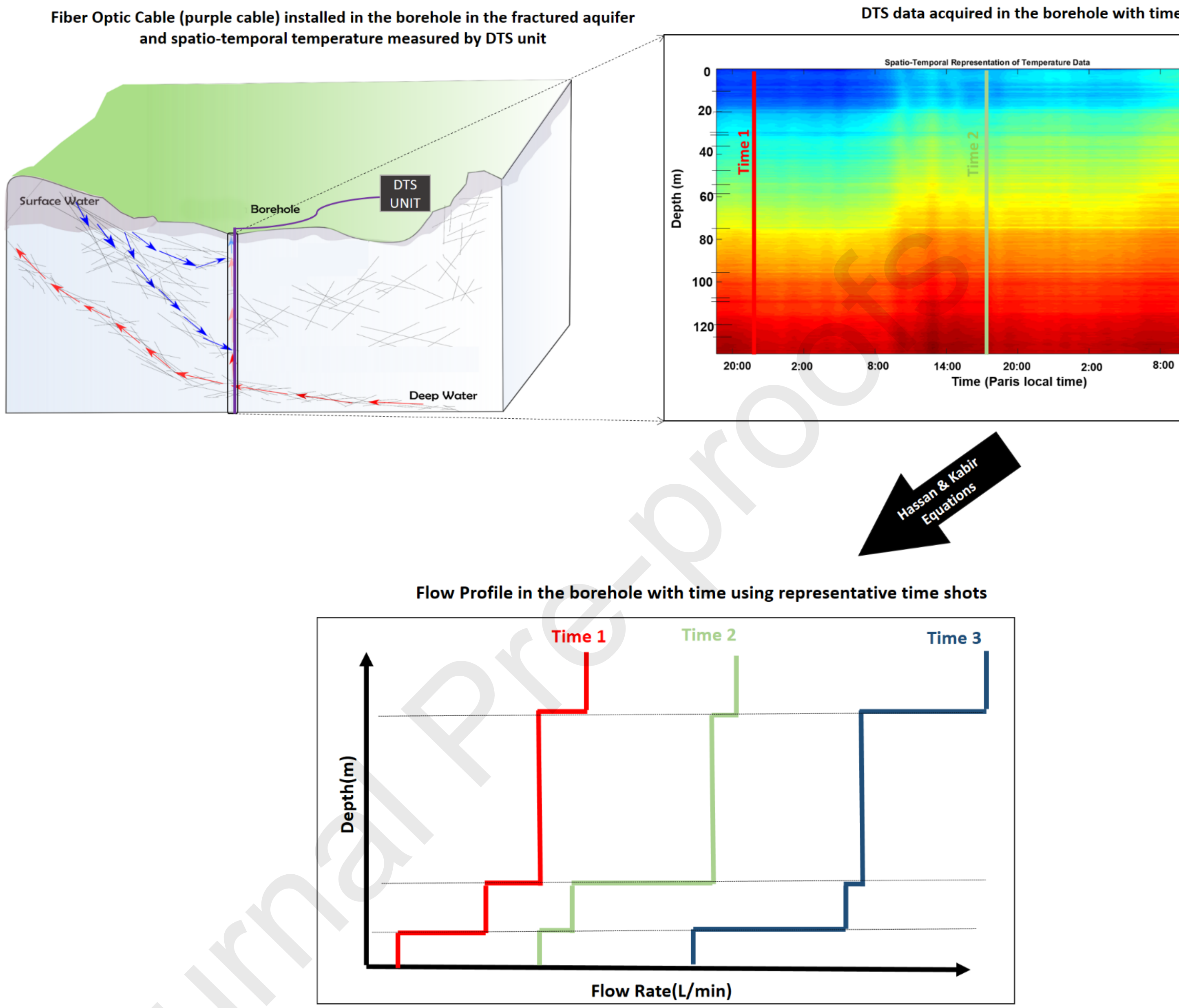

Highlights

- Distributed Temperature sensing (DTS) data are used to monitor the variations with time of borehole flows in the fractured media.

• A computationally fast tool, based on analytical solutions, is proposed to invert the temperature profile into flow profile across the borehole.

• We also show the potential of using DTS data for real time monitoring of dynamic behavior of fractured media at borehole scale.